CONFIDENTIAL

Copy 375
RM L56E23

NACA RM L56E23

NACA

CASE FILE
COPY

RESEARCH MEMORANDUM

STATIC LATERAL AND DIRECTIONAL STABILITY AND EFFECTIVE SIDEWASH CHARACTERISTICS OF A MODEL OF A 35° SWEPT-WING AIRPLANE AT A MACH NUMBER OF 1.61

By M. Leroy Spearman

Langley Aeronautical Laboratory
Langley Field, Va.

CLASSIFICATION CHANGED TO UNCLASSIFIED
AUTHORITY: NASA TECHNICAL PUBLICATIONS ANNOUNCEMENTS NO. 38
EFFECTIVE DATE: JANUARY 12, 1961 WHL

CLASSIFIED DOCUMENT

This material contains information affecting the National Defense of the United States within the meaning of the espionage laws, Title 18, U.S.C., Secs. 793 and 794, the transmission or revelation of which in any manner to an unauthorized person is prohibited by law.

NATIONAL ADVISORY COMMITTEE
FOR AERONAUTICS

WASHINGTON
August 28, 1956

CONFIDENTIAL

NATIONAL ADVISORY COMMITTEE FOR AERONAUTICS

RESEARCH MEMORANDUM

STATIC LATERAL AND DIRECTIONAL STABILITY AND EFFECTIVE SIDEWASH CHARACTERISTICS OF A MODEL OF A 35° SWEPT-WING AIRPLANE AT A MACH NUMBER OF 1.61

By M. Leroy Spearman

SUMMARY

Tests have been made in the Langley 4- by 4-foot supersonic pressure tunnel at a Mach number of 1.61 to determine the aerodynamic characteristics in sideslip at various angles of attack from 0° to about 16° for a 35° swept-wing fighter model.

The results indicated that a considerable portion of the vertical-tail contribution to the static directional stability was required to overcome the instability of the wing-body combination, and, because of a decrease in the tail contribution with increasing angle of attack, the configuration with the vertical tail on became unstable above about 8° angle of attack.

With increasing angle of attack, a destabilizing effective sidewash existed in the region of the tail for both the wing-on and wing-off arrangements but the effect was somewhat more pronounced with the wing off.

Some mutual interference effects resulting from the addition of the wing and vertical tail were indicated in that the existence of a large destabilizing effect that occurred for the wing-body combination was not apparent when the wing was added to the body-tail combination.

INTRODUCTION

At the present time, little information is available concerning the lateral and directional stability characteristics at combined angles of attack and sideslip for aircraft configurations at low supersonic Mach numbers. As pointed out in reference 1, aircraft designed for the

supersonic speed range are generally characterized by large bodies of high fineness ratio and far-rearward center-of-gravity positions. Such arrangements result in large unstable body moments and in a reduction in the vertical-tail contribution to directional stability. Hence, a large percentage of the tail contribution is required to overcome the body moment and only a small percentage is available to provide positive stability. Under such conditions, factors that affect the tail contribution, even to a slight degree, begin to assume greater importance.

In order to fill partially the need for information on directional characteristics at low supersonic speeds, an investigation has been conducted in the Langley 4- by 4-foot supersonic pressure tunnel in which the aerodynamic characteristics in sideslip were determined through an angle-of-attack range up to 16° for a 35° swept-wing fighter-airplane model at a Mach number of 1.61. The results of this investigation are presented herein.

Various combinations of component parts were tested in order to observe the effects of the wing, the vertical tail, and the horizontal tail on the lateral and directional stability. In addition, through the use of an offset or deflected vertical-tail installation, the vertical-tail effectiveness and the effective sidewash at the tail were determined.

SYMBOLS

The results are presented as coefficients of force and moments and are referred to the body-axis system. The moment reference point is at a body longitudinal station corresponding to the 25-percent mean-geometric-chord point of the wing. (See fig. 1.)

The symbols are defined as follows:

C_n	yawing-moment coefficient, Yawing moment/qSb
C_l	rolling-moment coefficient, Rolling moment/qSb
C_Y	side-force coefficient, Side force/qS
q	free-stream dynamic pressure
S	wing area
b	wing span

c	wing chord
$\bar{c}$	wing mean geometric chord
α	angle of attack, deg
β	angle of sideslip, deg
β_T	local angle of sideslip at vertical tail, deg
δ_v	vertical-tail deflection (trailing edge left when viewed from rear, positive), deg
σ	effective sidewash angle (positive when tending to increase positive side force at the tail), deg
$C_{n_{\delta_v}}$	rate of change of yawing-moment coefficient with vertical-tail deflection, $\partial C_n/\partial \delta_v$
$C_{l_{\delta_v}}$	rate of change of rolling-moment coefficient with vertical-tail deflection, $\partial C_l/\partial \delta_v$
$C_{Y_{\delta_v}}$	rate of change of side-force coefficient with vertical-tail deflection, $\partial C_Y/\partial \delta_v$
$\partial\sigma/\partial\beta$	rate of change of effective sidewash angle with angle of sideslip
C_{n_β}	rate of change of yawing-moment coefficient with angle of sideslip, $\partial C_n/\partial \beta$ at $\beta \approx 0^\circ$
C_{l_β}	rate of change of rolling-moment coefficient with angle of sideslip, $\partial C_l/\partial \beta$ at $\beta \approx 0^\circ$
C_{Y_β}	rate of change of side-force coefficient with angle of sideslip, $\partial C_Y/\partial \beta$ at $\beta \approx 0^\circ$
B	body
W	wing
H	horizontal tail
V	vertical tail

MODEL AND APPARATUS

A three-view drawing of the model is shown in figure 1 and the geometric characteristics of the model are presented in table I. A photograph of the model is shown as figure 2. The model had a wing with 35° of sweepback at the quarter-chord line and NACA 65A-series sections having thickness ratios varying from 6 percent at the root to 4 percent at the tip. The wing had a taper ratio of 0.5 and an aspect ratio of 4, and it was mounted in a semihigh position on the body. The horizontal tail was mounted below the extended chord plane of the wing and had an incidence angle of -3°.

The body was indented in the vicinity of the wing in accordance with the transonic area rule.

The vertical tail was designed so that it could be mounted on the model in the normal zero-deflection position or in a deflected position of 5° with the leading edge offset to the right. The vertical tail, horizontal tail, and wing could all be removed from the model in order to facilitate the testing of various combinations of component parts.

The model was equipped with side inlets but for all tests these inlets were plugged and faired into the body.

Forces and moments were measured by means of a six-component internal strain-gage balance and indicating system. The model was mounted on a rotary-type support strut that permitted testing at combined angles of attack and sideslip.

The tests were conducted in the Langley 4- by 4-foot supersonic pressure tunnel which is described in reference 2.

TESTS AND CORRECTIONS

Test Conditions

The tests were made at a Mach number of 1.61 and a Reynolds number of 1.56×10^6 based on the wing mean geometric chord. The stagnation dewpoint was maintained at -25° F or less, so that no condensation effects were encountered in the test section.

Tests were made through an angle-of-sideslip range from 0° to about 20° at nominal angles of attack of 0°, 4°, 8°, 12°, and 16°.

Corrections and Accuracy

The angles of attack and sideslip have been corrected for the deflections of the sting and balance due to the aerodynamic loads.

The estimated errors in the individual measured quantities are as follows:

C_n	±0.0002
C_l	±0.0003
C_Y	±0.0010
α, deg	±0.2
β, deg	±0.1

PRESENTATION OF RESULTS

The figures are presented in the following manner:

	Figure
Effect of vertical tail on the lateral stability characteristics of the body in sideslip	3
Effect of vertical tail on the lateral stability characteristics of the wing-body combination in sideslip	4
Effect of vertical tail and vertical-tail deflection on the lateral stability characteristics of the body—horizontal-tail combination in sideslip	5
Effect of vertical tail and vertical-tail deflection on the lateral stability characteristics of the wing—body—horizontal-tail combination in sideslip	6
Variation of sideslip derivatives with angle of attack for various configurations	7
Effect of angle of attack on vertical-tail effectiveness; horizontal tail on, $\beta = 0^\circ$	8
Vertical-tail control characteristics	9
Variation of effective sidewash angle with angle of attack	10

DISCUSSION

Basic Data

The basic data presented in figures 3 to 6 reveal some points of general interest. Of primary concern for configurations of the type

investigated is the large percentage of the vertical-tail contribution to the yawing moment that is required to overcome the unstable moment of the tail-off configurations even at $\alpha = 0^\circ$. (See fig. 3(a), for example.) Under such conditions, as pointed out in reference 1, any losses in vertical-tail contribution that might result from aeroelastic effects, from control deflections, or from wing-body wake and sidewash effects with increasing angle of attack become exceedingly important and may lead to directional instability. As indicated by the results for various angles of attack (figs. 3 to 6), the losses in tail contribution do lead to regions of static directional instability above about 8° angle of attack.

Because of a decrease in tail contribution with increasing angle of sideslip and, to some extent, because of increasing instability of the body, the variation of C_Y and C_n with β for the vertical tail-on configurations in the low α range is quite nonlinear and the yawing moment C_n does, in fact, reverse toward the unstable range. Such a condition would result in sensitive directional control since some deflections of a rudder, for example, would provide two trim points in sideslip.

Another nonlinear variation of interest is that which occurs for C_n and C_Y at small angles of sideslip and high angles of attack for those configurations having no wing or vertical tail (B and BH). For these wing-off configurations, the addition of the vertical tail at the highest angle of attack appears to be destabilizing at small sideslip angles (figs. 3(e) and 5(e)). When the wing is added (compare figs. 3(e) and 4(e), for example), the addition of the vertical tail is always stabilizing.

This nonlinear trend in C_n and C_Y at high angles of attack and small sideslip angles for the body and body—horizontal-tail configuration may result from body vorticity effects or from changes in the afterbody pressure distribution.

Sideslip Derivatives

The variations of the sideslip derivatives with angle of attack as obtained from the basic data of figures 3 to 6 are presented in figure 7 for all combinations of components. The flagged symbols and dashed fairings are used to denote the configurations with the vertical tail removed.

One of the most noticeable characteristics is the rapid increase in $-C_{Y_\beta}$ and decrease in $-C_{n_\beta}$ for the configurations with both wing and vertical tail off (B and BH) between $\alpha \approx 8^\circ$ and $\alpha \approx 15^\circ$. The

addition of the vertical tail to these configurations at the highest angle of attack indicates a loss in $-C_{Y_\beta}$ and a slight destabilizing increment of C_{n_β}. The contribution of the vertical tail to C_{l_β} for the wing-off configurations decreases rapidly with increasing angle of attack but at the highest angle of attack the contribution is still negative. Hence, there is some indication that complete loss or reversal of tail load does not occur and that the losses indicated by C_{Y_β} and C_{n_β} probably include changes in the fuselage afterbody load as well.

With the wing installed, the changes in C_{n_β} and C_{Y_β} with α for the vertical-tail-off configurations are less pronounced, and the increment provided by installation of the vertical tail, although progressively decreasing, is always stabilizing. The contribution of the vertical tail to C_{l_β} for the wing-on configurations also decreases slightly with increasing angle of attack. These characteristics are essentially the same both with and without the horizontal tail.

Thus, it appears that there are some compensating effects resulting from the addition of the wing and tail. The destabilizing effect of the wing on the vertical-tail-off configurations at high angles of attack, for example, is not apparent for the tail-on configurations and all configurations having a vertical tail have essentially the same variation of C_{n_β} throughout the angle-of-attack range.

Effects of Vertical-Tail Deflection

A 5° deflection of the vertical tail, as might be expected, provided rather large positive increments of C_l and C_Y and negative increments of C_n for both the wing-on and wing-off cases (figs. 5 and 6). The variations of C_n, C_l, and C_Y with angle of attack at $\beta = 0^\circ$ for $\delta_v = 0^\circ$ and 5° are presented in figure 8(a) for the wing-on case and in figure 8(b) for the wing-off case.

With the assumption that C_n, C_l, and C_Y vary linearly with δ_v between 0° and 5°, the values of $C_{n_{\delta_v}}$, $C_{l_{\delta_v}}$, and $C_{Y_{\delta_v}}$ were obtained from figure 8 and are presented in figure 9. The control characteristics are essentially constant with angle of attack except at the higher angles where some decrease in $C_{n_{\delta_v}}$ is indicated for the wing-off configuration.

Estimated values of $C_{Y_{\delta_v}}$, $C_{l_{\delta_v}}$, and $C_{n_{\delta_v}}$ at $\alpha = 0^\circ$ (fig. 9) are in reasonably close agreement with the experimental results. These estimated values are based on a lift-curve slope for the exposed portion of the vertical tail that was obtained through the use of reference 3. The moment values were obtained by assuming that the vertical-tail side force was acting at the quarter chord of the exposed-vertical-tail mean geometric chord.

Effective Sidewash Characteristics

Through the use of the deflected-vertical-tail results, the variation of the effective sidewash angle σ with angle of sideslip was obtained. The relation $\sigma = \beta - \beta_T$ was used where β_T is the local angle of sideslip of the vertical tail. The local angle of sideslip of the vertical tail is assumed to be zero at those angles of airplane sideslip for which the deflected vertical tail would provide no change in force or moment from that provided by the tail-off configuration. These tail angles were interpolated between the curves for $\delta_v = 0^\circ$ and $\delta_v = 5^\circ$ with the assumption, of course, that the tail force and moment would vary linearly with tail deflection. The results (fig. 10) indicate a small stabilizing sidewash variation $-\partial\sigma/\partial\beta$ up to about $\alpha = 6^\circ$ for both the wing-on and wing-off configurations. Above $\alpha = 6^\circ$ the effective sidewash becomes increasingly destabilizing for both cases but is considerably more destabilizing for the wing-off configuration than for the wing on.

CONCLUSIONS

Tests made to determine the aerodynamic characteristics in sideslip through an angle-of-attack range from 0° to about 16° for a model of a 35° swept-wing fighter airplane at a Mach number of 1.61 indicated the following conclusions:

1. A considerable portion of the vertical-tail contribution to the static directional stability was required to overcome the unstable moment of the tail-off configurations, and, because of a decrease in the tail contribution with increasing angle of attack, the configuration with the vertical tail on became unstable above about 8° angle of attack.

2. With increasing angle of attack, an increasingly destabilizing effective sidewash existed at the tail for both the wing-on and wing-off arrangements but the effect was somewhat greater with the wing off.

3. Some mutually beneficial interference effects resulting from the addition of the wing and vertical tail to the body were indicated in that the existence of a large destabilizing effect that occurred for the wing-body combination was not apparent when the wing was added to the body-tail combination.

Langley Aeronautical Laboratory,
National Advisory Committee for Aeronautics,
Langley Field, Va., May 9, 1956.

REFERENCES

1. Spearman, M. Leroy, and Henderson, Arthur, Jr.: Some Effects of Aircraft Configuration on Static Longitudinal and Directional Stability at Supersonic Mach Numbers Below 3. NACA RM L55L15a, 1956.

2. Spearman, M. Leroy, and Hilton, John H., Jr.: Aerodynamic Characteristics at Supersonic Speeds of a Series of Wing-Body Combinations Having Cambered Wings With an Aspect Ratio of 3.5 and a Taper Ratio of 0.2. Effects of Sweep Angle and Thickness Ratio on the Static Lateral Stability Characteristics at M = 1.60. NACA RM L51K15a, 1952.

3. Harmon, Sidney M., and Jeffreys, Isabella: Theoretical Lift and Damping In Roll of Thin Wings With Arbitrary Sweep and Taper at Supersonic Speeds - Supersonic Leading and Trailing Edges. NACA TN 2114, 1950.

TABLE I.- GEOMETRIC CHARACTERISTICS OF MODEL

Wing:

Area, sq ft	1.113
Span, in.	25.31
Aspect ratio	4.0
Taper ratio	0.5
Root chord, in.	8.44
Tip chord, in.	4.22
Mean geometric chord, in.	6.6
Root section	NACA 65A006
Tip section	NACA 65A004
Sweep, c/4 line, deg	35

Horizontal tail:

Area, sq ft	0.2913
Span, in.	12.12
Aspect ratio	3.5
Taper ratio	0.4
Root chord, in.	4.942
Tip chord, in.	1.978
Mean geometric chord, in.	3.67
Root section	NACA 65A006
Tip section	NACA 65A004
Sweep, c/4 line, deg	35

Vertical tail:

Area (theoretical), sq ft	0.178
Area (exposed), sq ft	0.152
Span (theoretical), in.	6.20
Span (exposed), in.	5.7
Aspect ratio (theoretical)	3.0
Aspect ratio (exposed)	2.97
Taper ratio (theoretical)	0.177
Taper ratio (exposed)	0.174
Root chord (theoretical), in.	7.0
Root chord (exposed), in.	6.46
Mean geometric chord (exposed), in.	4.45
Tip chord, in.	1.24
Root section (theoretical)	NACA 65A006
Tip section	NACA 65A004
Sweep, c/4 line, deg	44.4

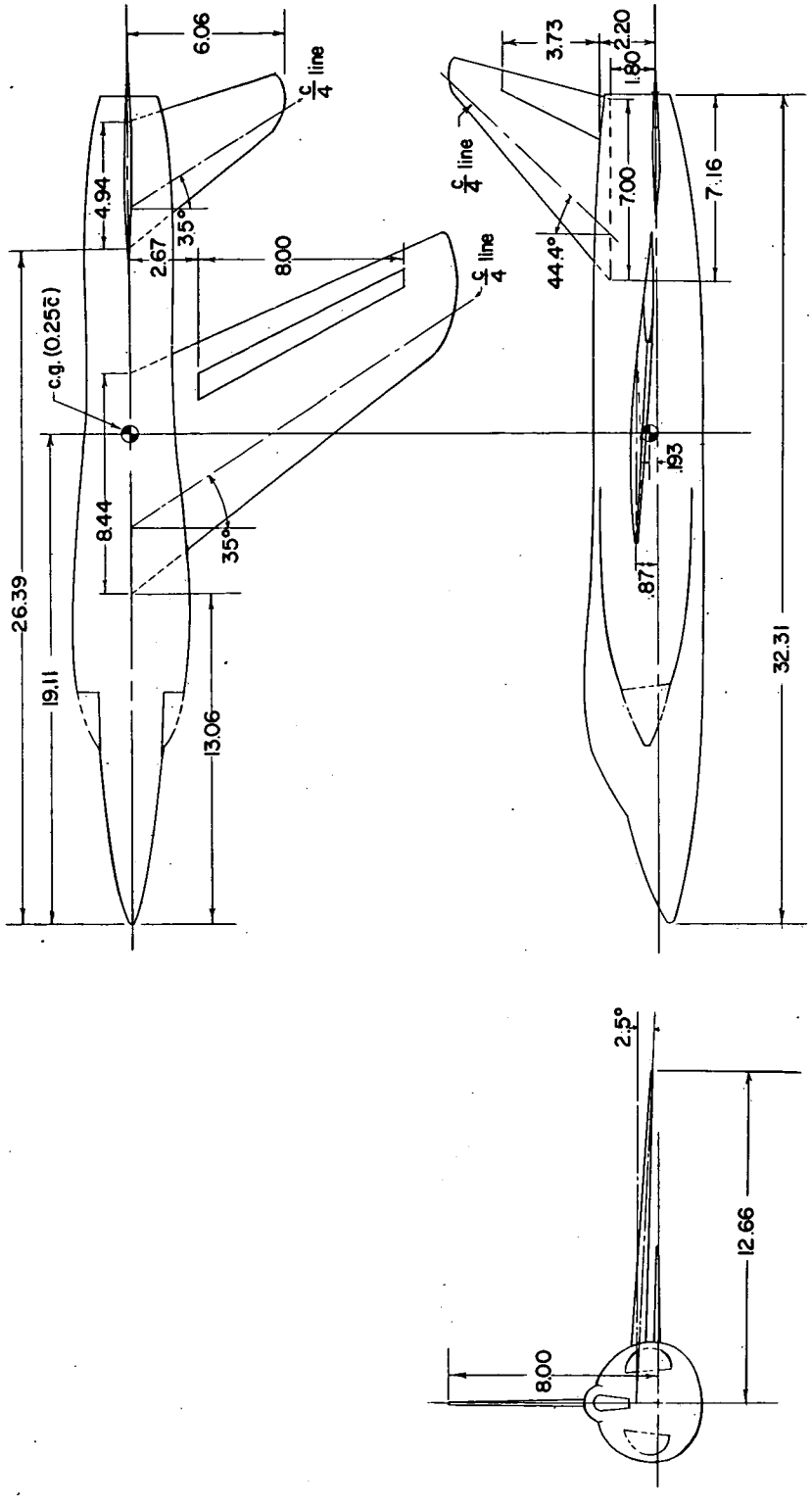
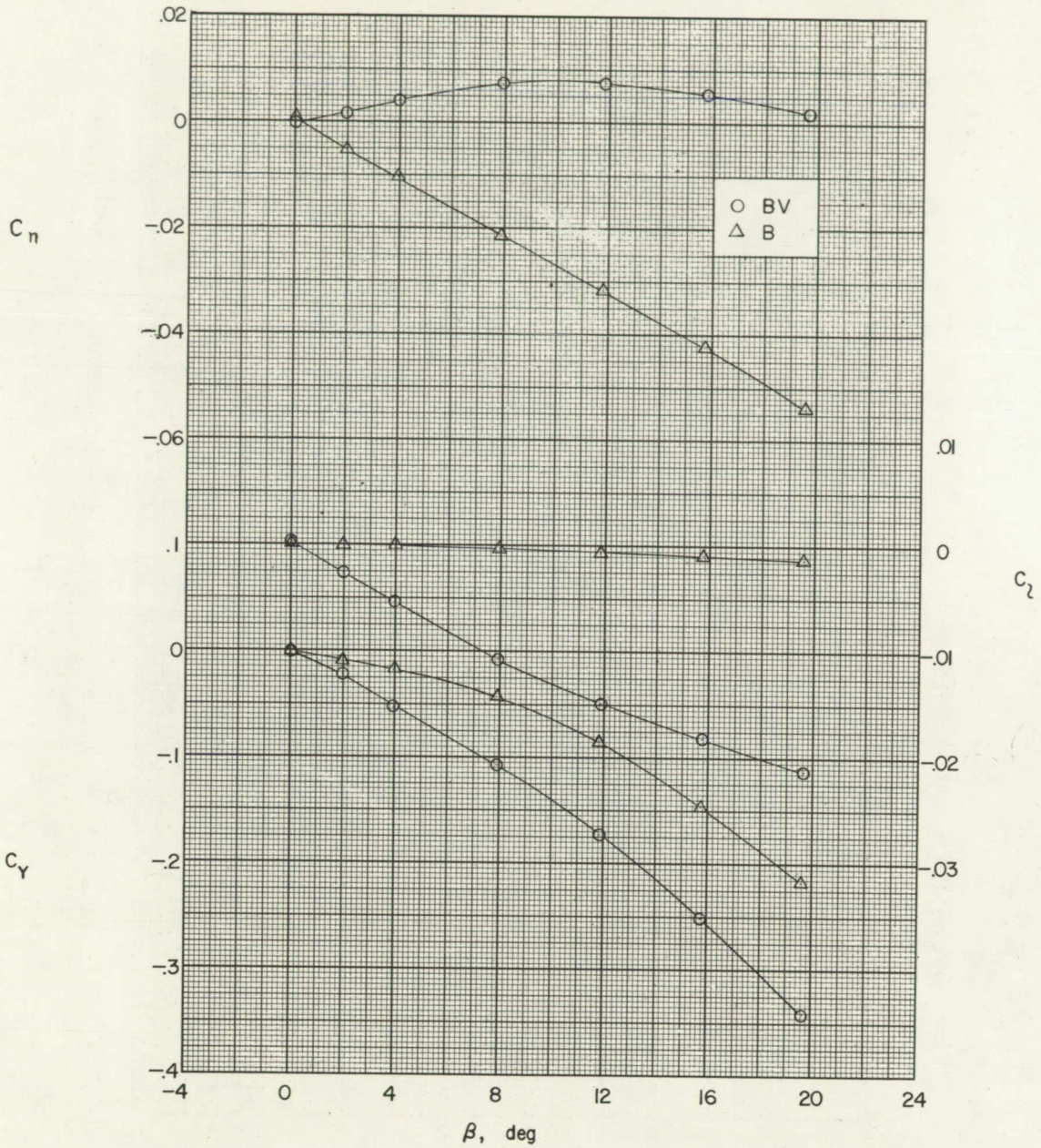


Figure 1.- Three-view drawing of model. All dimensions are in inches unless otherwise indicated.



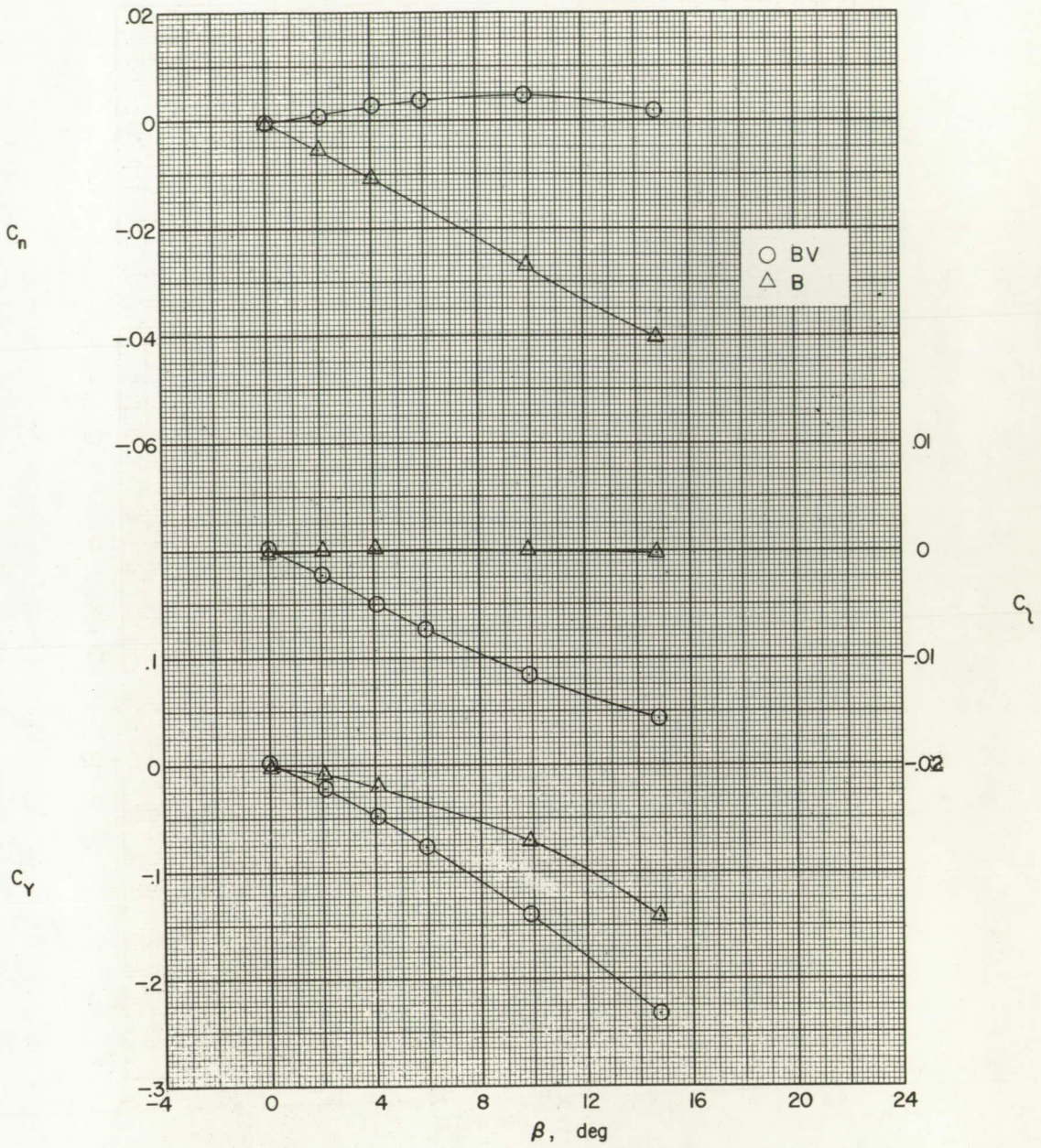
L-88318

Figure 2.- Model of 35° swept-wing airplane tested.



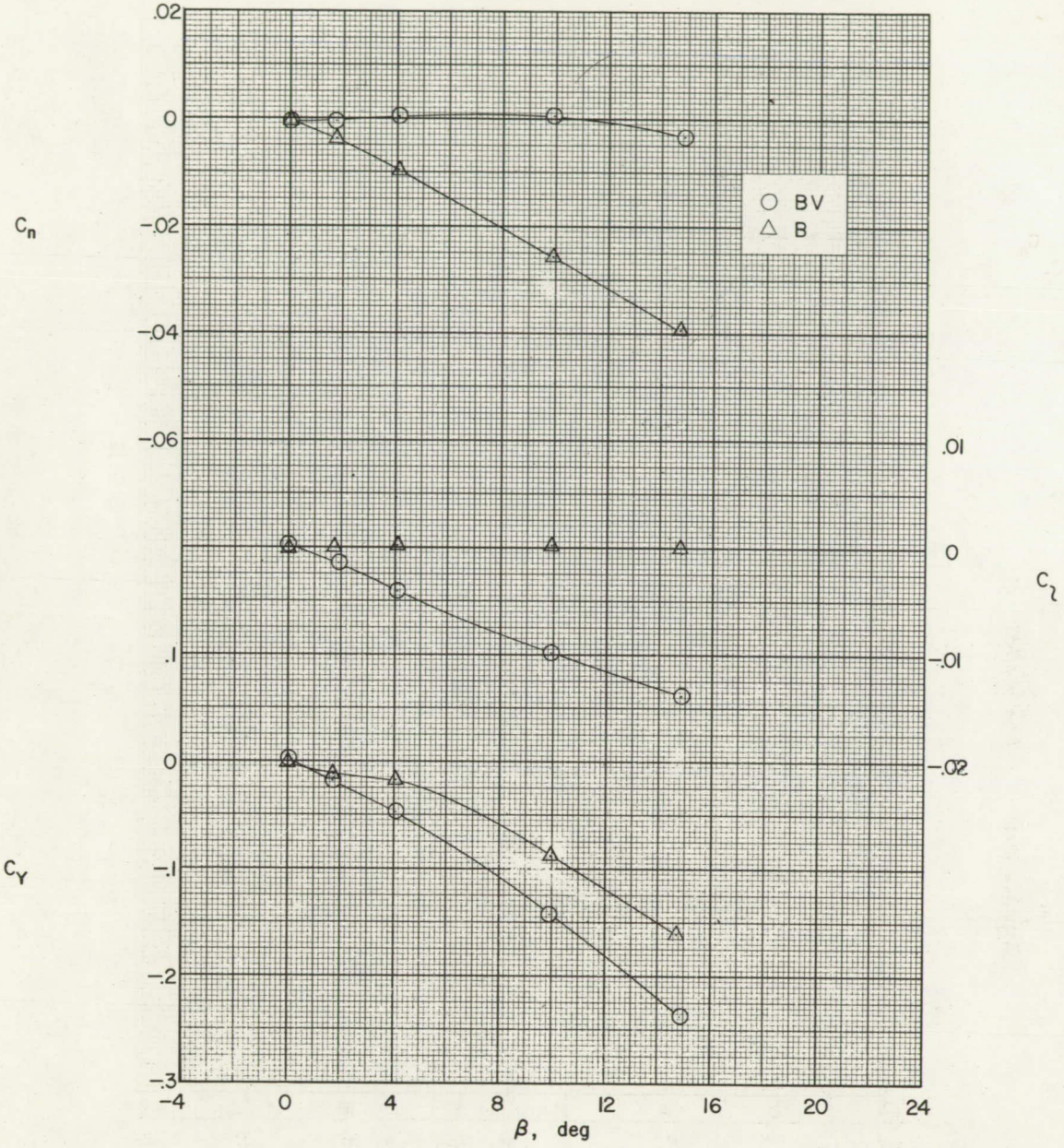
(a) $\alpha = 0^\circ$.

Figure 3.- Effect of vertical tail on the lateral stability characteristics of the body in sideslip.



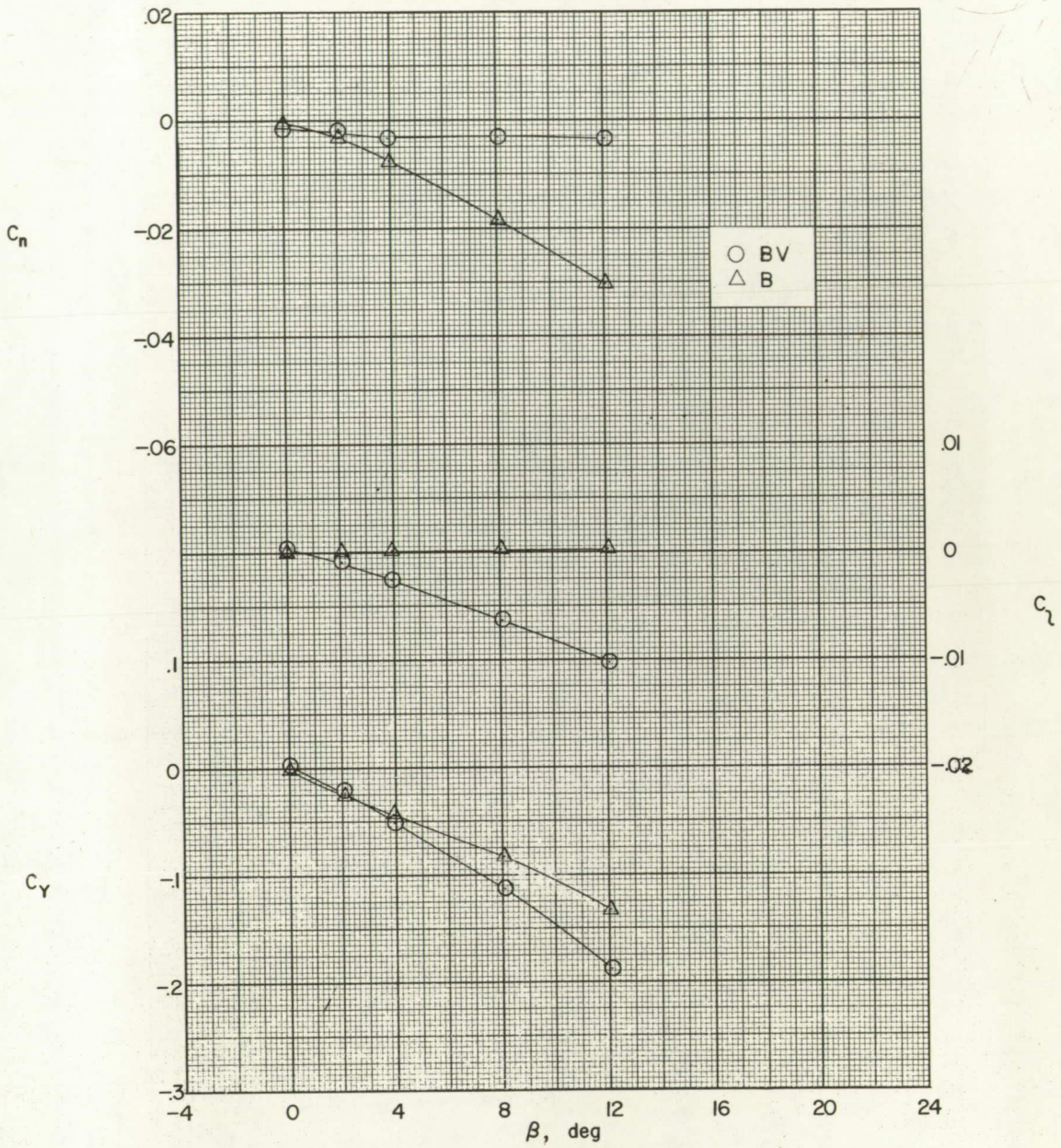
(b) $\alpha = 4^{\circ}$.

Figure 3.- Continued.



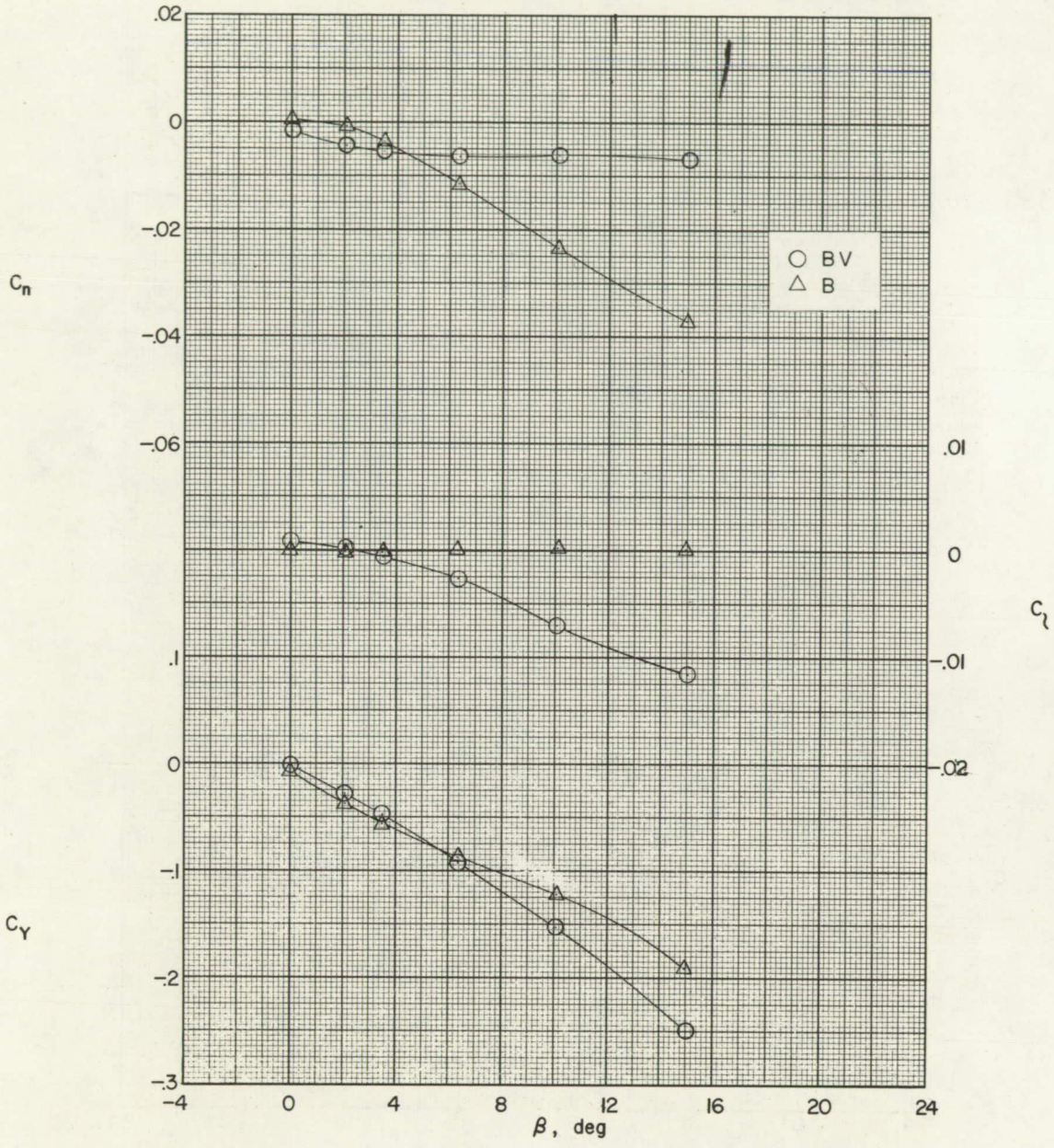
(c) $\alpha = 8.2^{\circ}$.

Figure 3.- Continued.



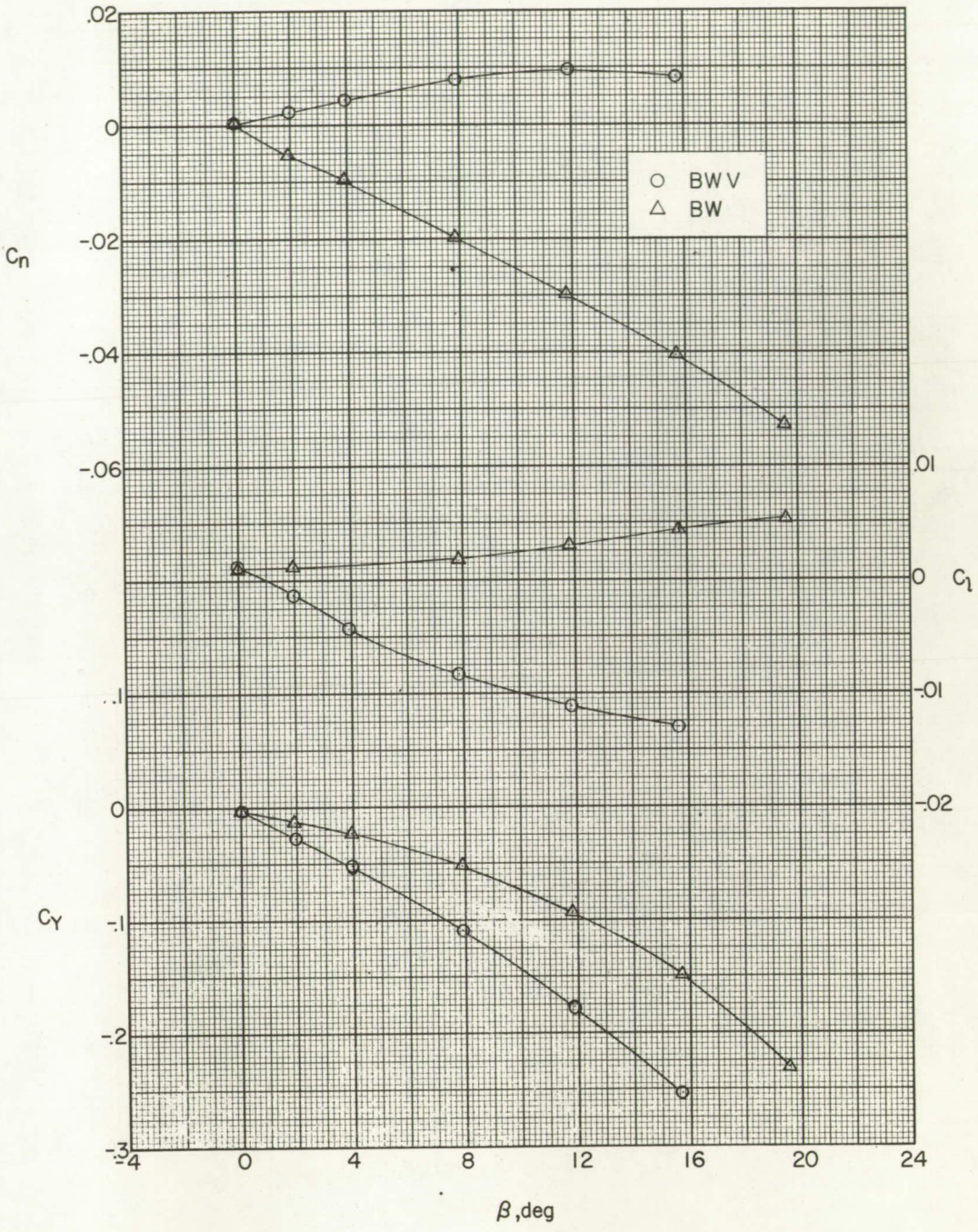
(d) $\alpha = 12^{\circ}$.

Figure 3.- Continued.



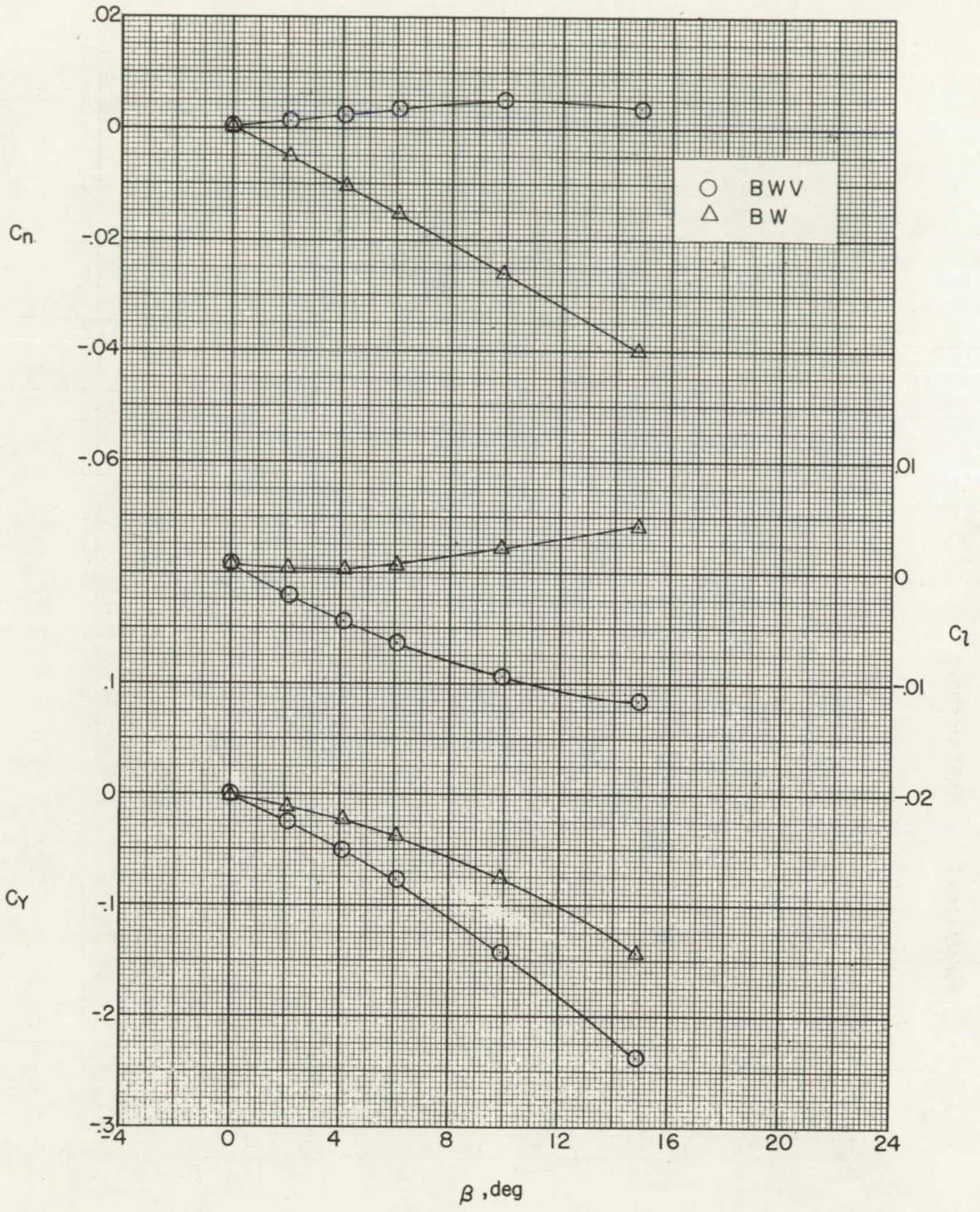
(e) $\alpha = 15.6^{\circ}$.

Figure 3.- Concluded.



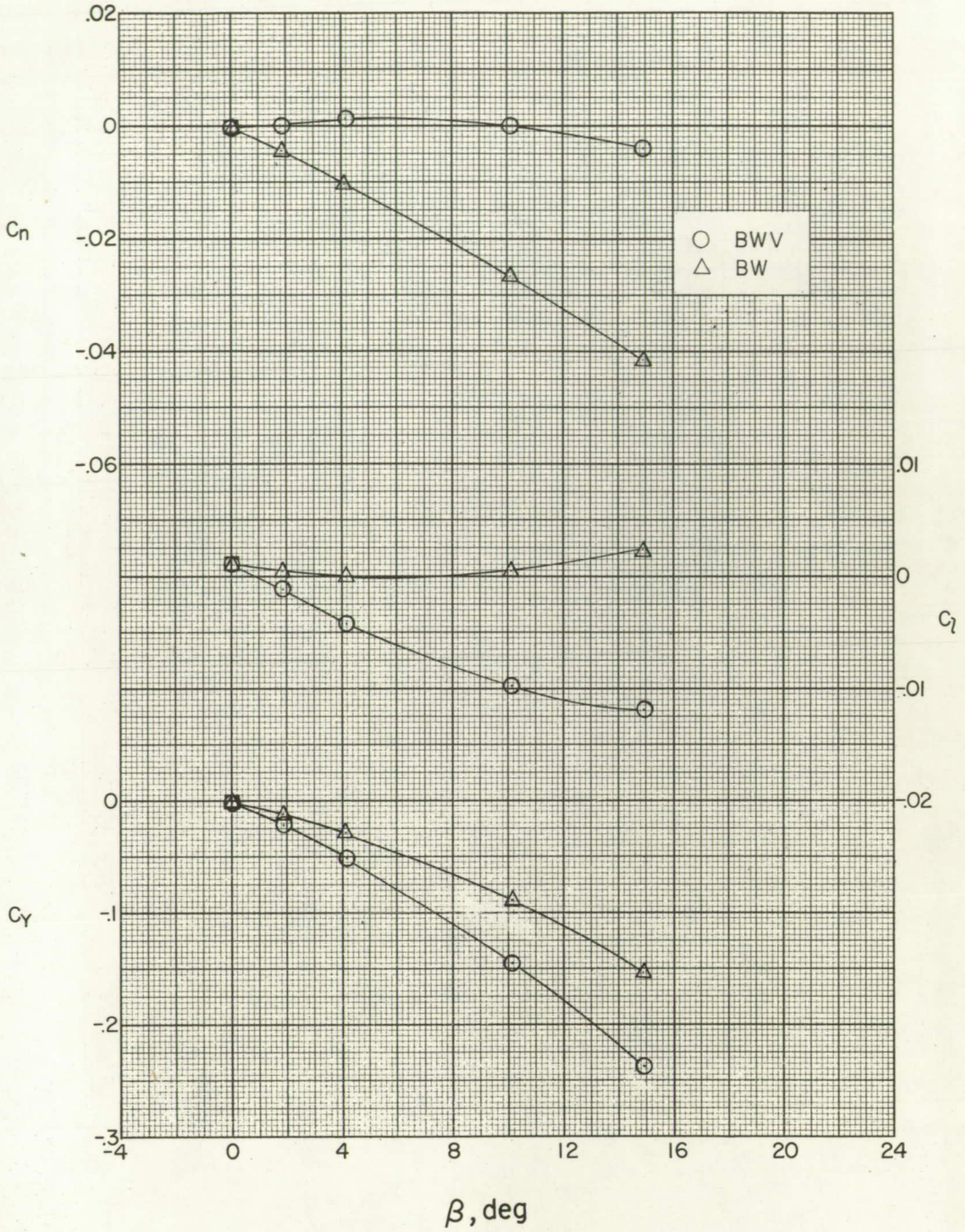
(a) $\alpha = 0^{\circ}$.

Figure 4.- Effect of vertical tail on the lateral stability characteristics of the wing-body combination in sideslip.



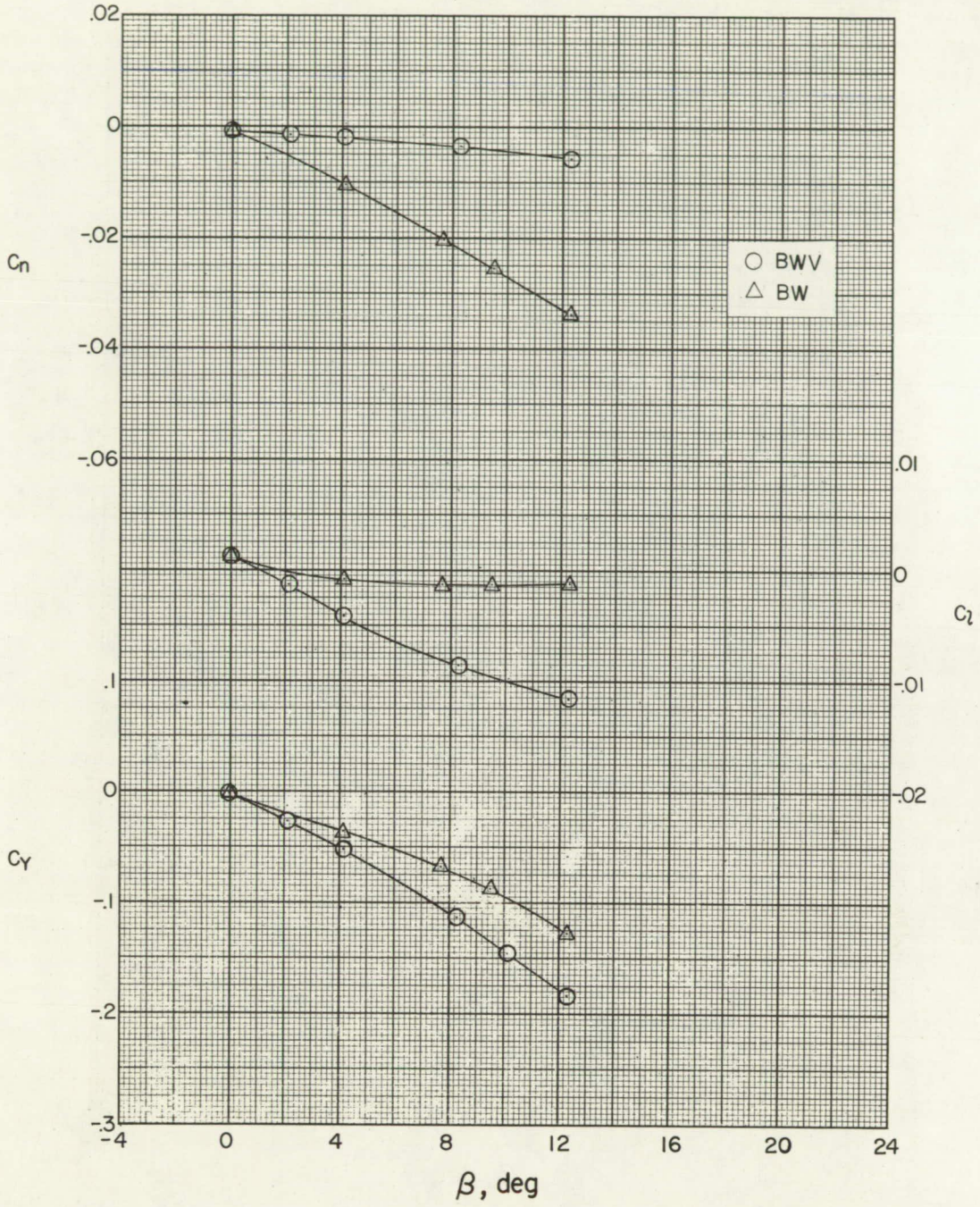
(b) $\alpha = 4^{\circ}$.

Figure 4.- Continued.



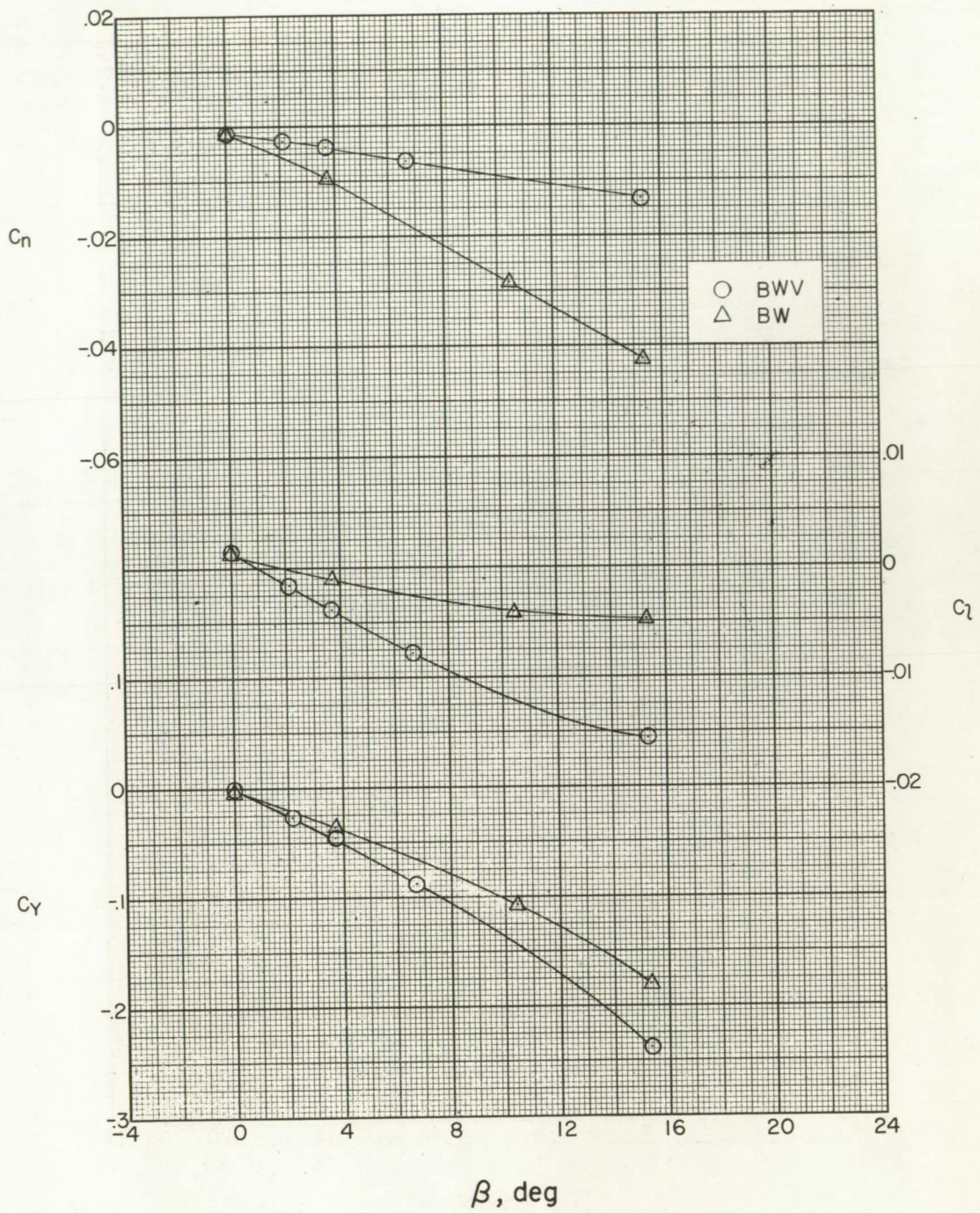
(c) $\alpha = 8.2^{\circ}$.

Figure 4.- Continued.



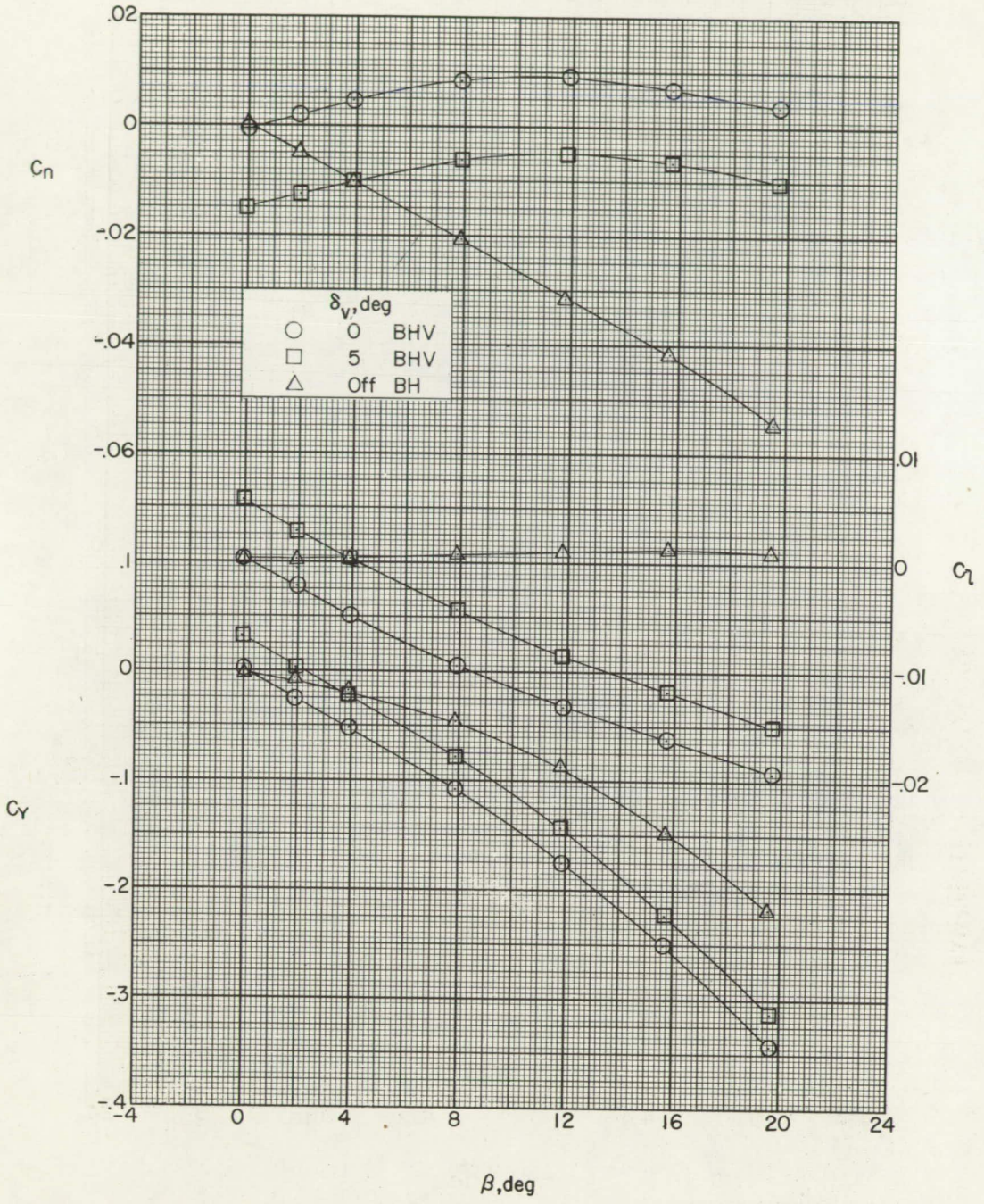
(d) $\alpha = 12^{\circ}$.

Figure 4.- Continued.



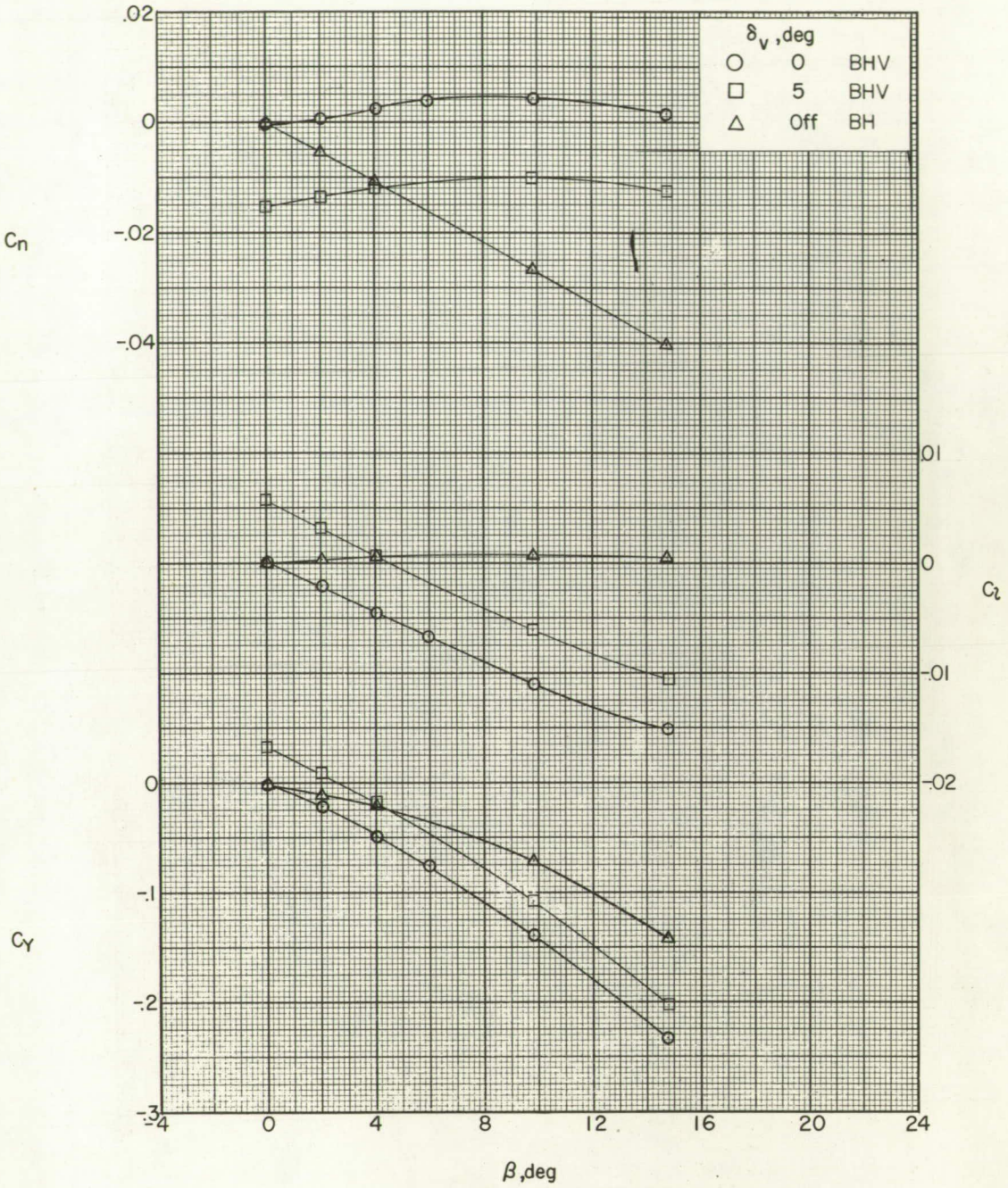
(e) $\alpha = 15.6^{\circ}$.

Figure 4.- Concluded.



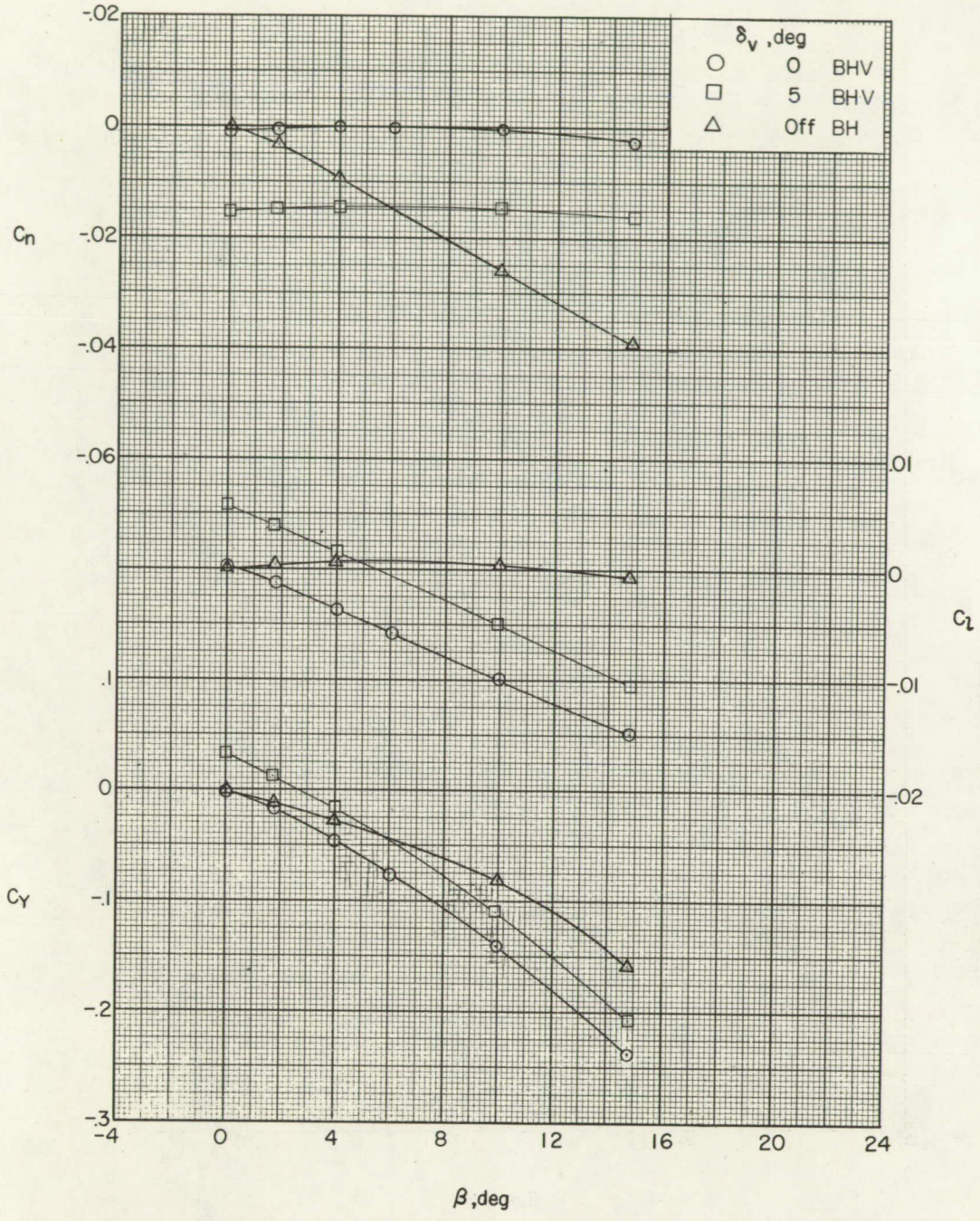
(a) $\alpha = 0^\circ$.

Figure 5.- Effect of vertical tail and vertical-tail deflection on the lateral stability characteristics of the body—horizontal-tail combination in sideslip.



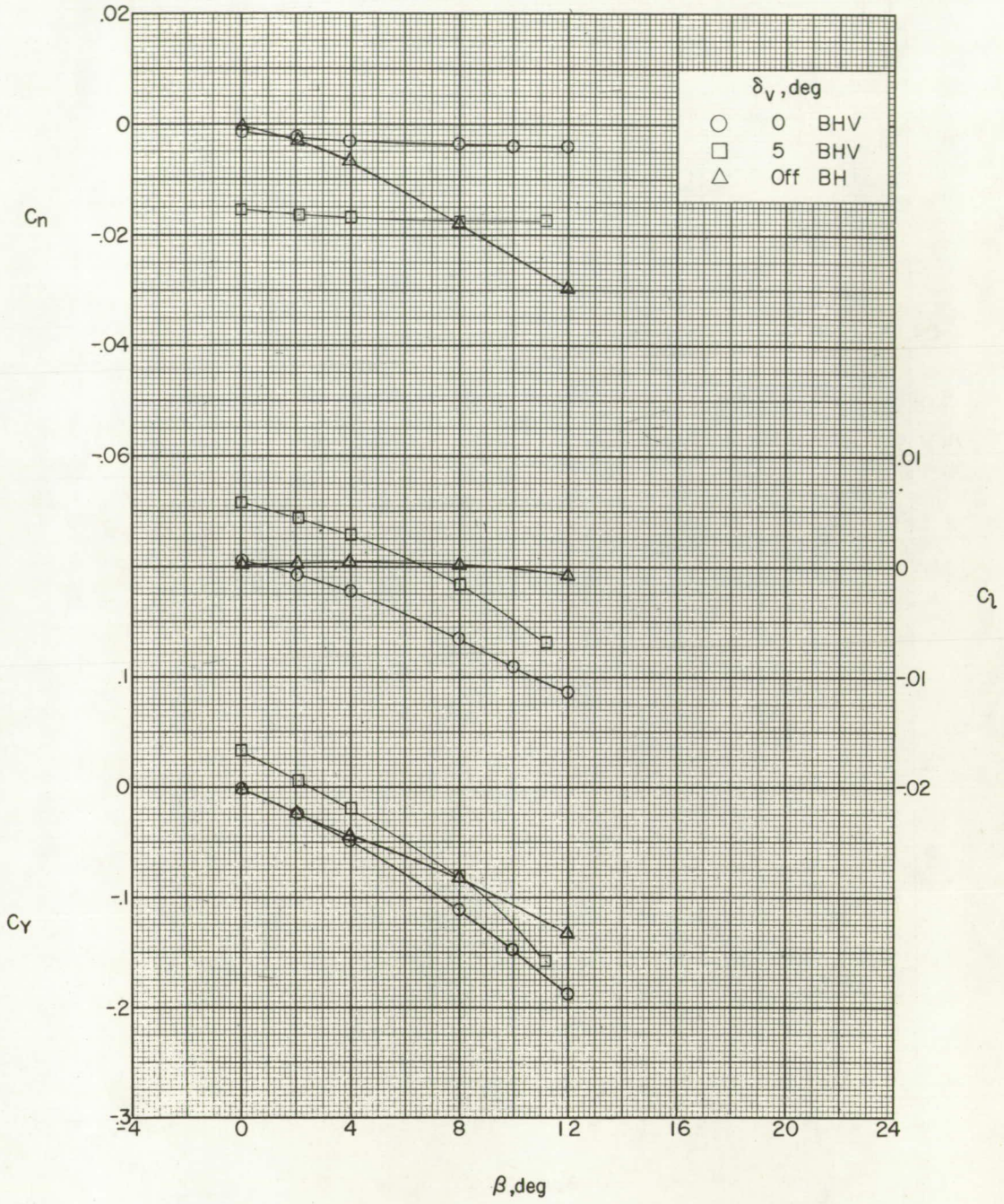
(b) $\alpha = 4^{\circ}$.

Figure 5.- Continued.



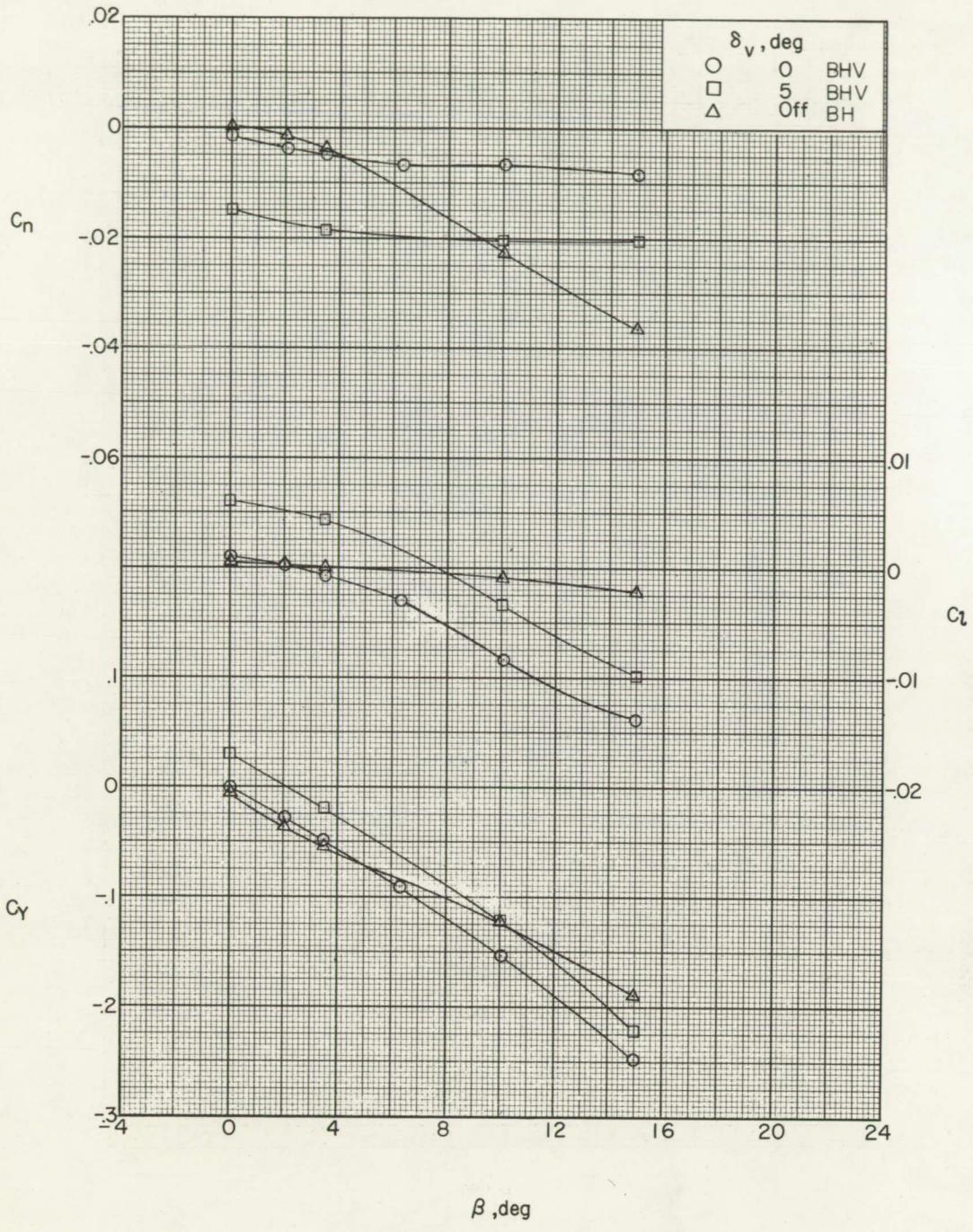
(c) $\alpha = 8^{\circ}$.

Figure 5.- Continued.



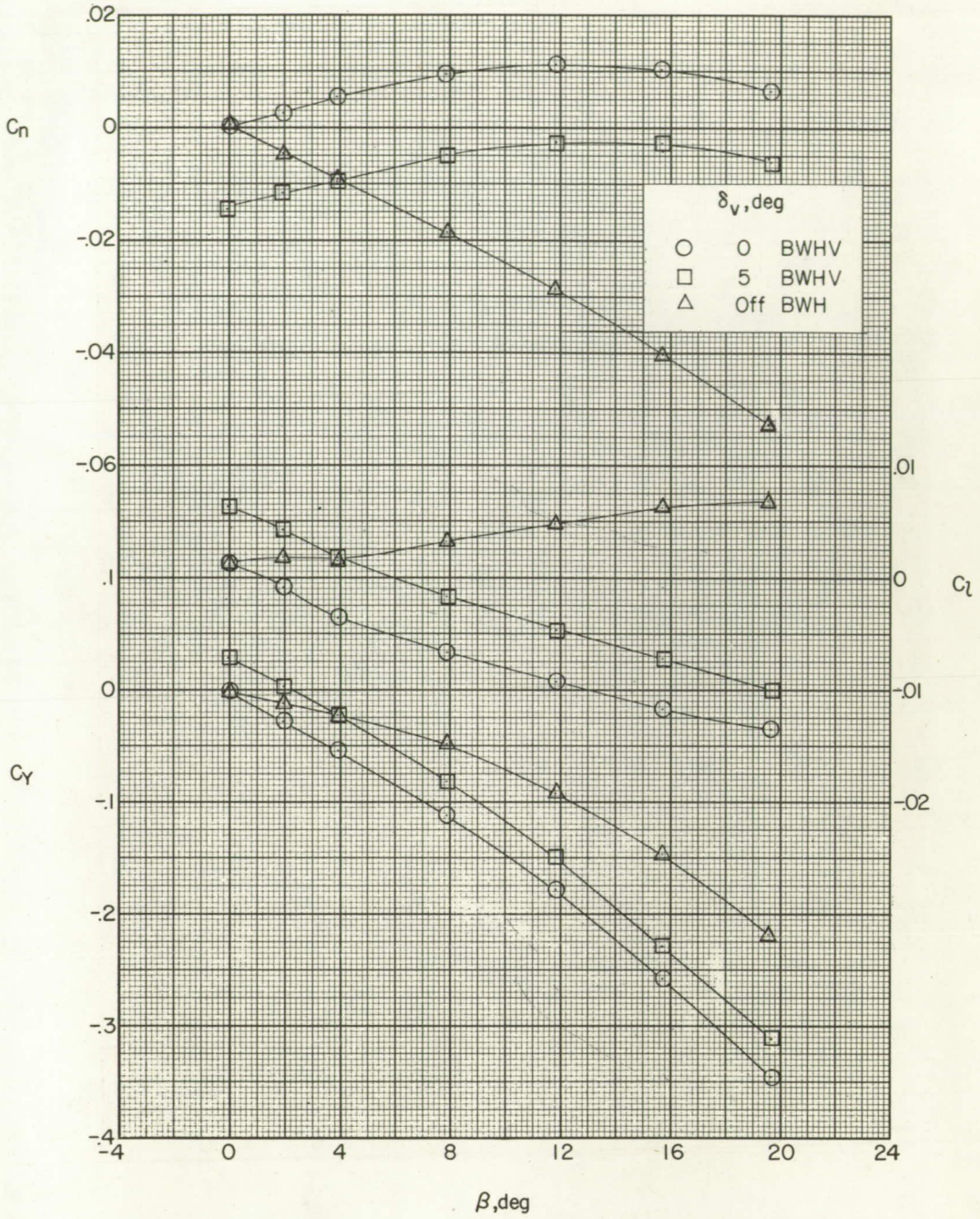
(d) $\alpha = 12^{\circ}$.

Figure 5.- Continued.



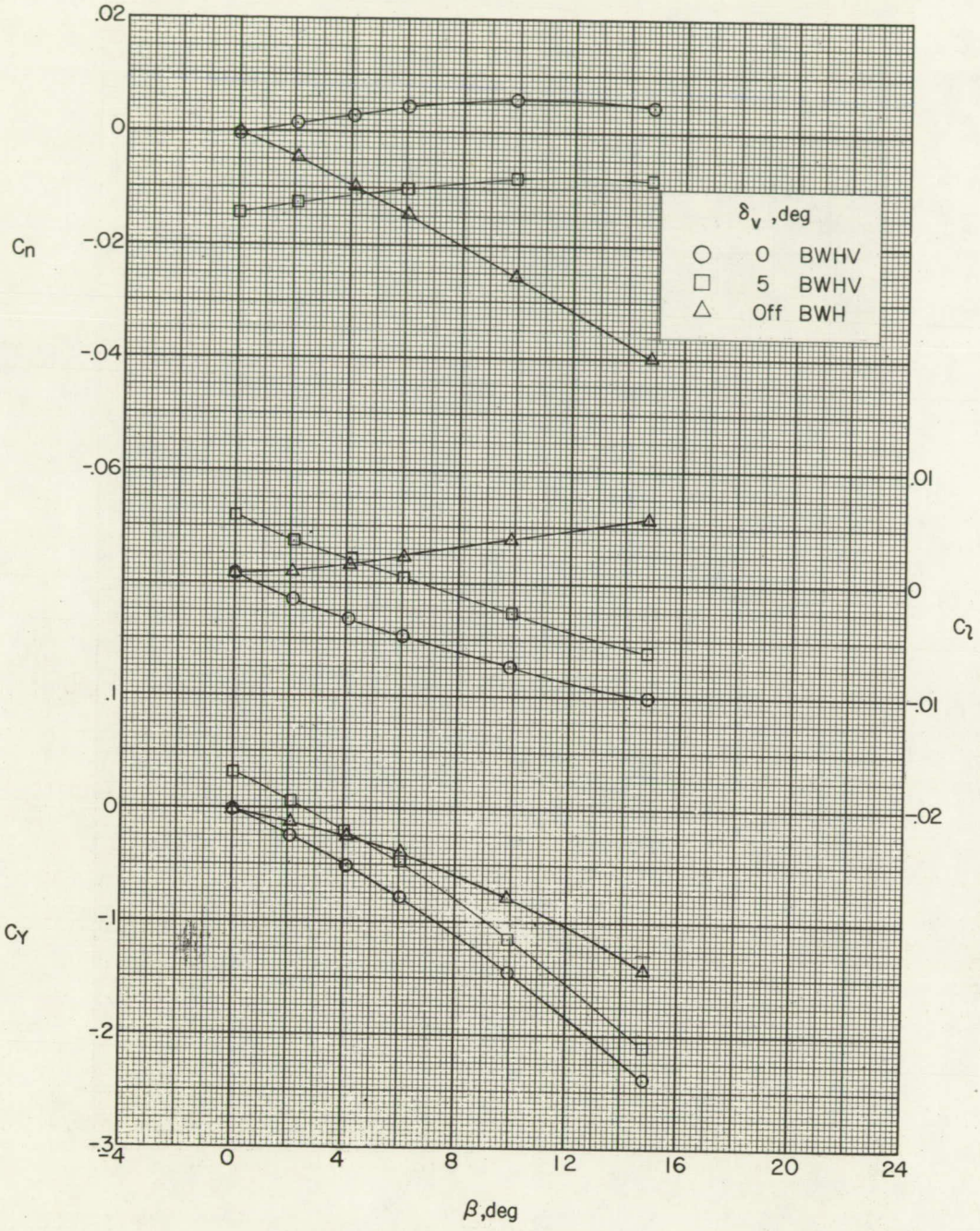
(e) $\alpha = 15^{\circ}$.

Figure 5.- Concluded.



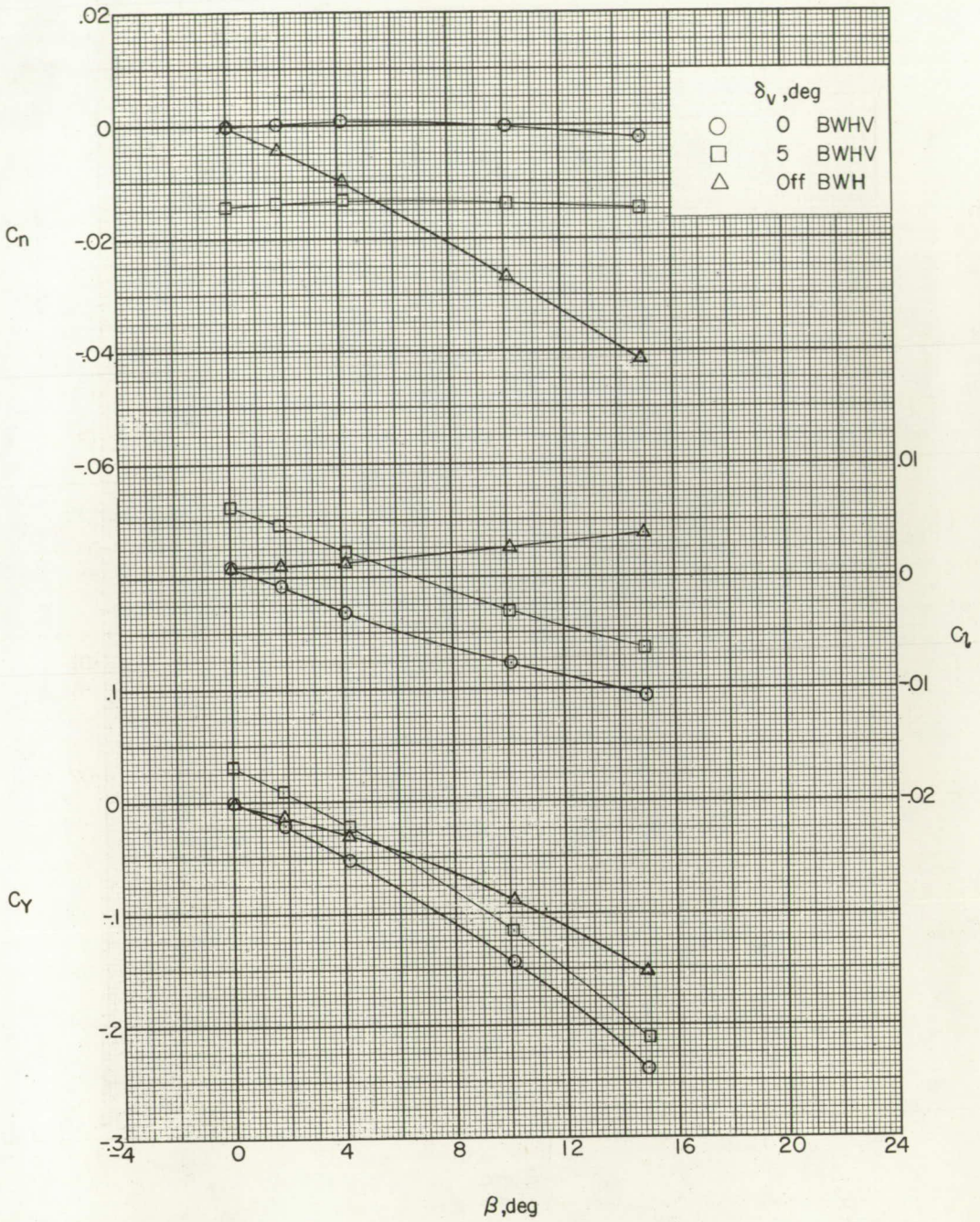
(a) $\alpha = 0^\circ$.

Figure 6.- Effect of vertical tail and vertical-tail deflection on the lateral stability characteristics of the wing—body—horizontal-tail combination in sideslip.



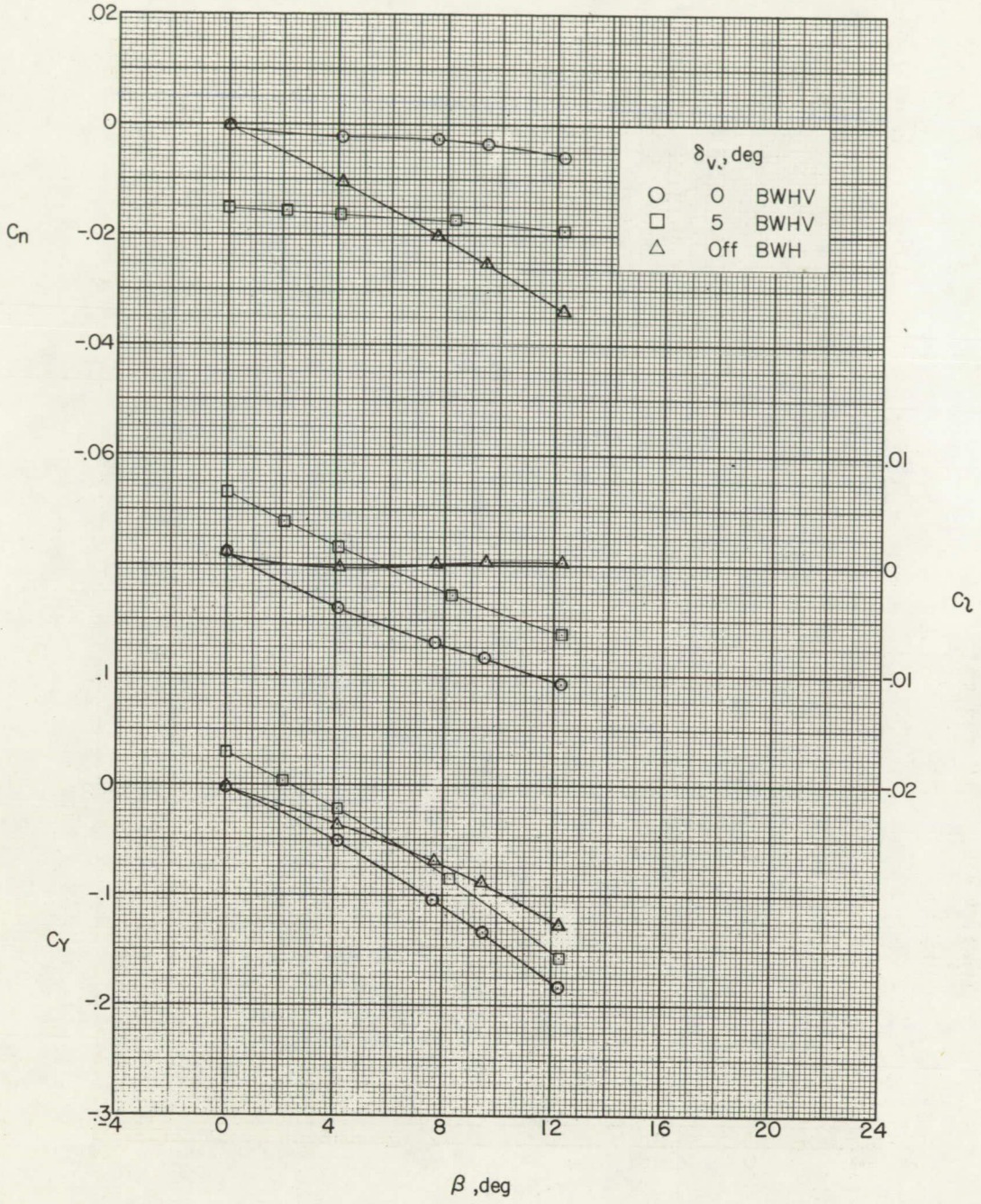
(b) $\alpha = 4^{\circ}$.

Figure 6.- Continued.



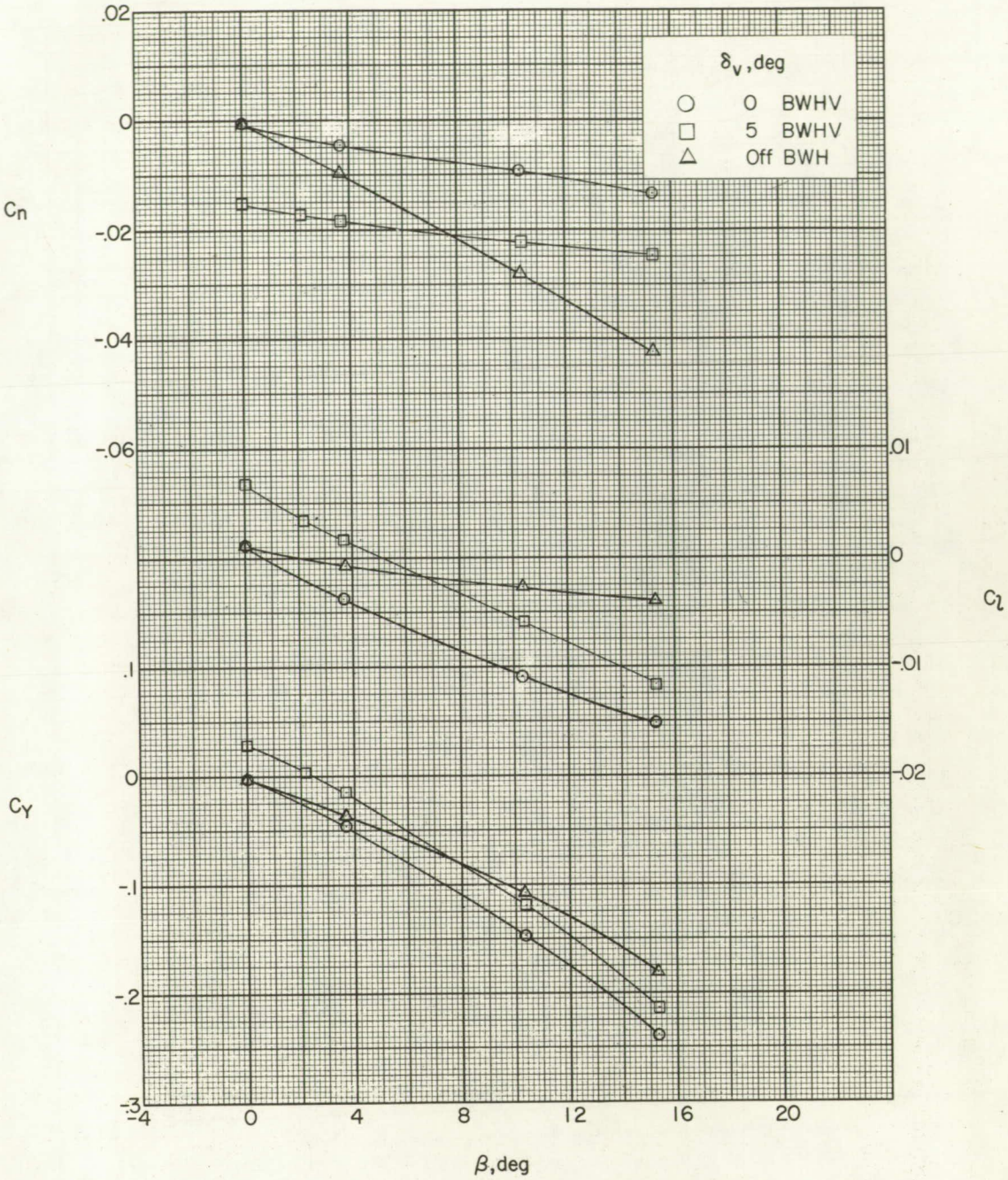
(c) $\alpha = 8.2^{\circ}$.

Figure 6.- Continued.



(d) $\alpha = 12^{\circ}$.

Figure 6.- Continued.



(e) $\alpha = 15.6^{\circ}$.

Figure 6.- Concluded.

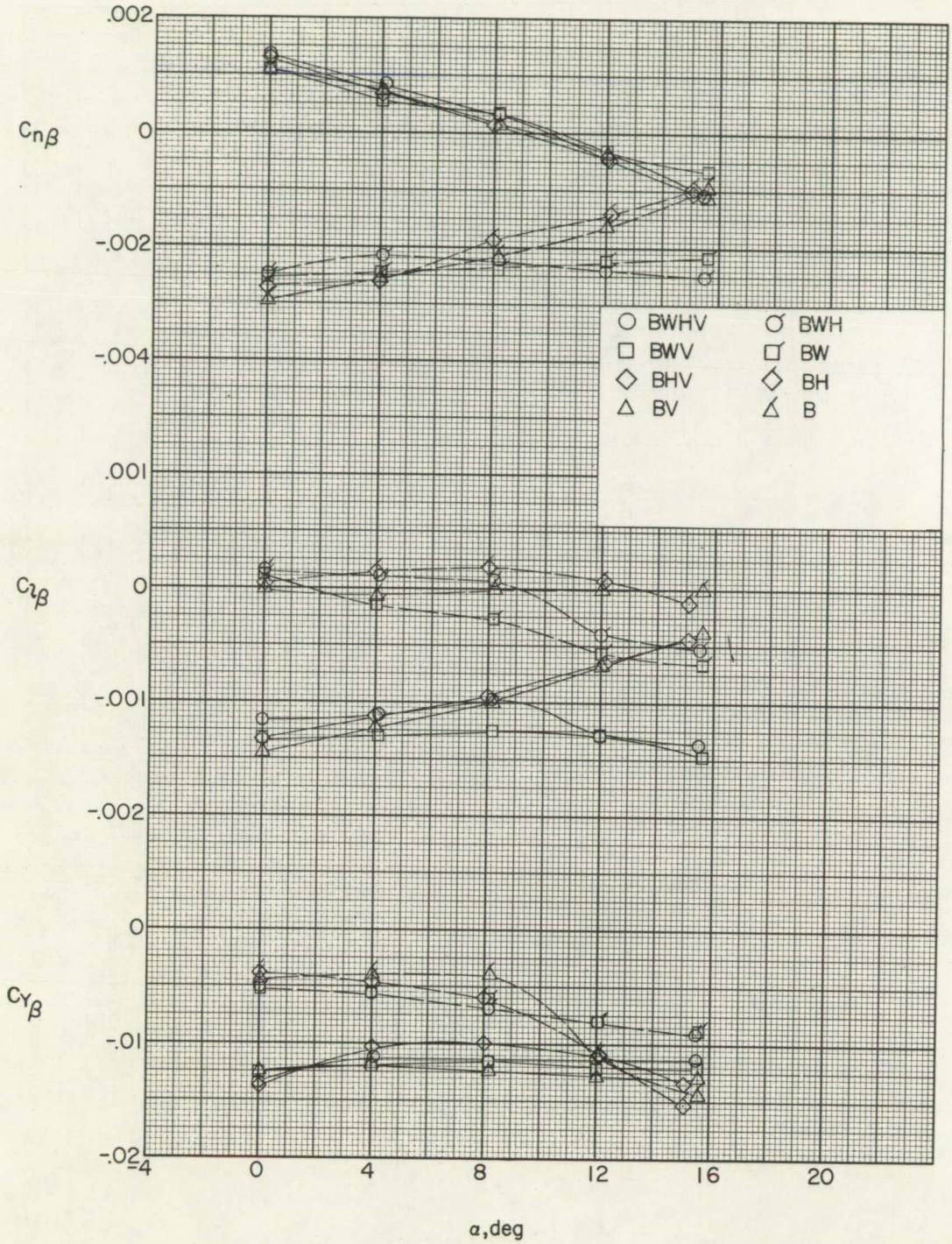
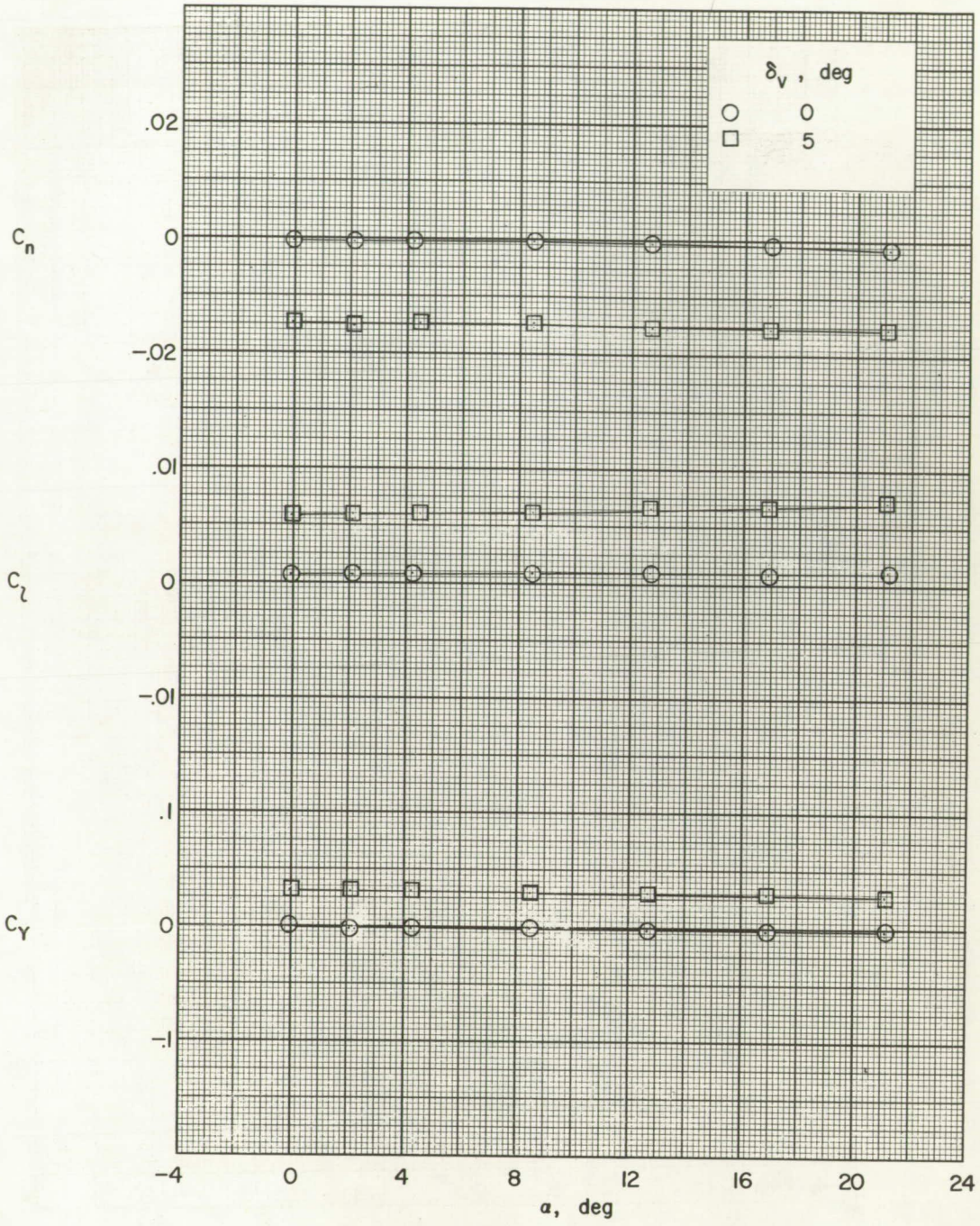
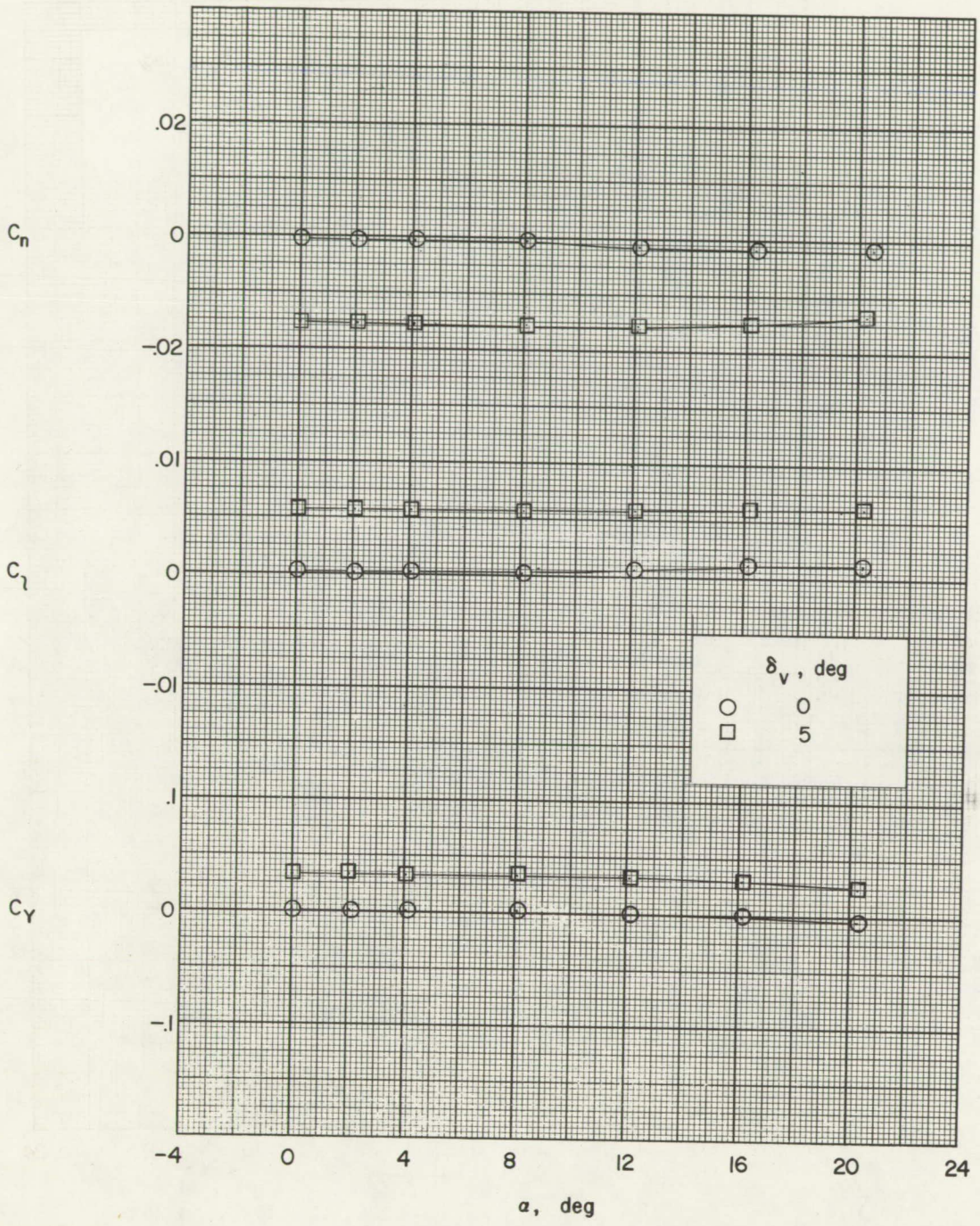


Figure 7.- Variation of sideslip derivatives with angle of attack for various configurations.



(a) Wing on.

Figure 8.- Effect of angle of attack on vertical-tail effectiveness. Horizontal tail on; $\beta = 0^{\circ}$.



(b) Wing off.

Figure 8.- Concluded.

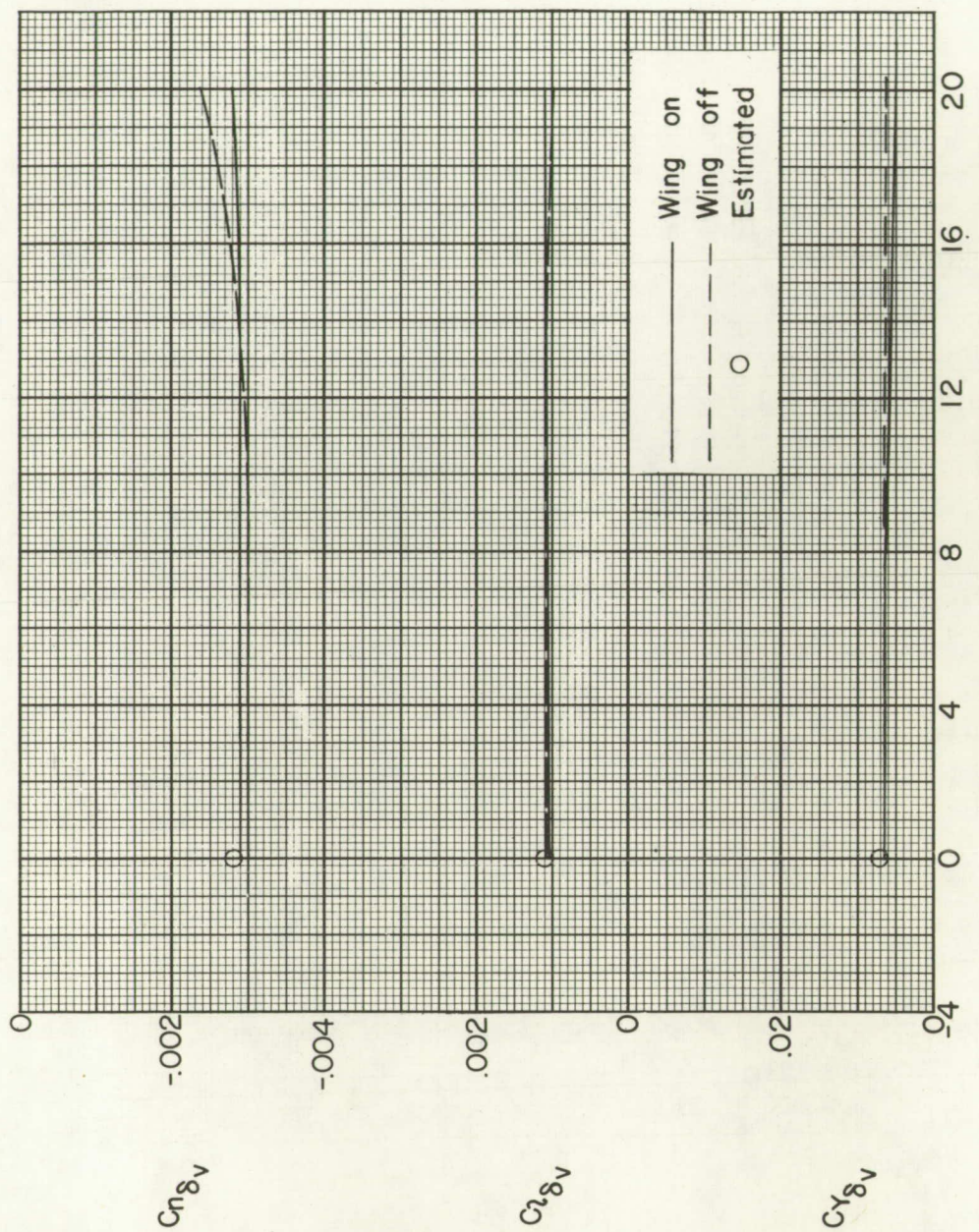


Figure 9.- Vertical-tail control characteristics.

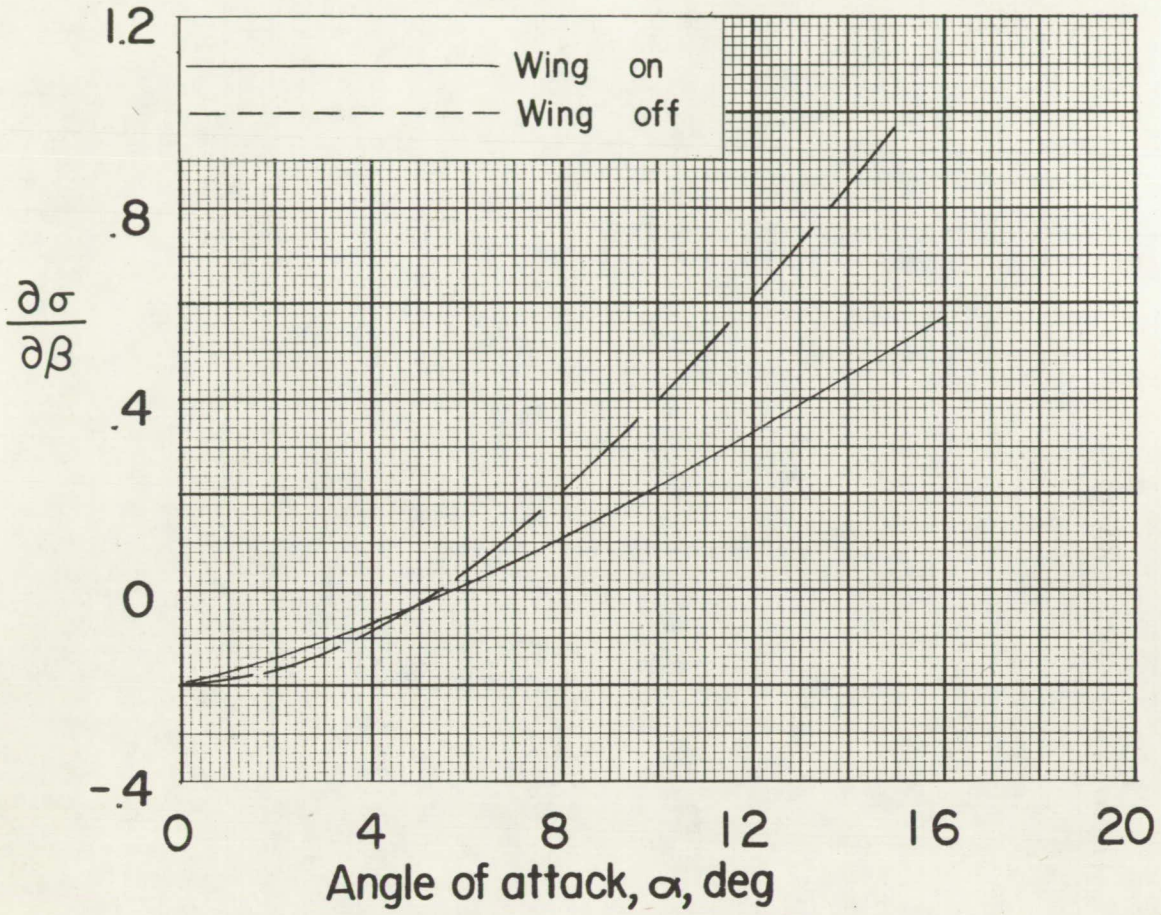


Figure 10.- Variation of effective sidewash angle with angle of attack.

NACA - Langley Field, Va.